

# Dispersion (asymptotic) theory of charged particle transfer reactions at low energies and nuclear astrophysics: I. the “non-dramatic” case

R. Yarmukhamedov,<sup>1\*</sup> and K. I. Tursunmakhatov<sup>2</sup>

April 4, 2020

<sup>1</sup>*Institute of Nuclear Physics, 100214 Tashkent, Uzbekistan*

<sup>2</sup>*Gulistan State University, 120100 Gulistan, Uzbekistan*

## Abstract

A new dispersion (asymptotic) theory is proposed for the peripheral sub- and above-barrier charged particle transfer  $A(x,y)B$  reaction in the three-body ( $A$ ,  $a$  and  $y$ ) model where  $x = y + a$  and  $B = A + a$ , and  $a$  is a transferred particle. It is based on the combination of the dispersion theory and the conventional DWBA method. The explicit forms have been derived for the exact three-body pole amplitude and differential cross section in which the contribution of the three-body ( $A$ ,  $a$  and  $y$ ) Coulomb dynamics of the transfer mechanism in the peripheral partial amplitudes, corresponding to partial waves with  $l_i \gg 1$ , is taken into account correctly. For the specific peripheral proton and triton transfer reactions, the comparative analysis of the peripheral partial amplitudes at  $l_i \gg 1$ , which correspond to the one-step pole and exact three-body pole amplitudes as well as those of the “post”-approximation and the post form of the conventional DWBA, is performed with each other. It shows the absolute inapplicability of the “post”-approximation usually applied for getting an information about specific asymptotic normalization coefficients being astrophysical interest.

PACS: 25.60 Je; 26.65.+t

---

\*Corresponding author, E-mail: rakhim@inp.uz

## I. INTRODUCTION

In the last two decades, a number of methods of analysis of experimental data for different nuclear processes were proposed to obtain information on the “indirect determined” (“experimental”) values of the specific asymptotic normalization coefficients (or respective nuclear vertex constants (NVC)) with the aim of their application to nuclear astrophysics (see, for example, Refs. [1–6] and the available references therein). One of such methods uses the modified DWBA [7, 8] for peripheral nuclear transfer reactions in which the differential cross section (DCS) is parametrized in the terms of the asymptotic normalization coefficients. One notes that an asymptotic normalization coefficient (ANC), which is proportional to the NVC for the virtual decay  $B \rightarrow A + a$ , determines the amplitude of the tail of the overlap function corresponding to the wave function of nucleus  $B$  in the binary ( $A + a$ ) channel (denoted by  $A + a \rightarrow B$  everywhere below) [9]. As the ANC for  $A + a \rightarrow B$  determines the probability of the configuration  $A + a$  in nucleus  $B$  at distances greater than the radius of nuclear  $Aa$  interaction, the ANC arises naturally in expressions for the cross sections of the peripheral nuclear reactions between charged particles at low energies, in particular, of the peripheral exchange  $A(B, A)B$ , transfer  $A(x, y)B$  and nuclear-astrophysical  $A(a, \gamma)B$  reactions.

In the present work, the peripheral charged particle transfer reaction

$$x + A \longrightarrow y + B \tag{1}$$

is considered in the framework of the three-body ( $A$ ,  $a$  and  $y$ ) model, where  $x=(y + a)$  is a projectile,  $B=(A + a)$  and  $a$  is a transferred particle. The main idea of consideration is based on the following two assumptions: i) the peripheral reaction (1) is governed by the singularity of the reaction amplitude at  $\cos \theta = \xi > 1$ , where  $\xi$  is the nearest to physical ( $-1 \leq \cos \theta \leq 1$ ) region singularity generated by the pole mechanism (Fig. 1a) [10] and  $\theta$  is the center-of-mass scattering angle; ii) the dominant role played by this nearest singularity is the result of the peripheral nature of the considered reaction at least in the angular range of the main peak of the angular distribution [11]. Consequently, it is necessary to know the behavior of the reaction amplitude at the nearest singularity  $\xi$  [12, 13], which in turn defines the behavior of the true peripheral partial amplitudes at  $l_i \gtrsim L_0 \gg 1$  ( $L_0 \sim k_i R_i^{\text{ch}}$  with  $R_i^{\text{ch}} \gtrsim R_N$ ) [14] giving the dominant contribution to the reaction amplitude at least in the angular range of the main peak of the angular distribution [11, 15], where  $l_i$ ,  $k_i$ ,  $R_i^{\text{ch}}$  and  $R_N$  are a partial wave, a number wave (or a relative momentum), a channel radius and the radius of the nuclear interaction of the colliding nuclei, respectively.

In practice, the “post”-approximation and the post form of the modified DWBA [7, 8] are used for the analysis of the specific peripheral proton transfer reactions. They are restricted by the zero- and first-order terms of the perturbation theory over the optical Coulomb polarization potential  $\Delta V_f^C$  (or  $\Delta V_i^C$ ) in the transition operator, respectively, which are sandwiched by the initial and final state wave functions in the matrix element of the reaction (1). At this, it is assumed that the contribution of the first-order term over  $\Delta V_f^C$  (or  $\Delta V_i^C$ ) to the matrix element is small [8]. But, it was shown in Refs. [2, 13, 16, 17] that, when the residual nuclei  $B$  are formed in weakly bound states being astrophysical interest, this assumption is not guaranteed for the

peripheral charged particle transfer reactions and, so, the extracted “experimental” ANC values may not have the necessary accuracy for their astrophysical application (see, for example, [17] and Table 1 in [2]). In this case, in the transition operator an inclusion of all other orders (the second and higher orders) of the power expansion in a series over  $\Delta V_f^C$  (or  $\Delta V_i^C$ ) is required for the DWBA cross section calculations since they strongly change the power of the peripheral partial amplitudes at  $l_i \gg 1$  [13, 17].

For these reasons, it is of great interest to derive the expressions for the amplitude and the differential cross section (DCS) of the peripheral reaction (1) within the so-called hybrid theory: the DWBA approach and the dispersion peripheral model [11, 12]. The main advantage of the hybrid theory as compared to the modified DWBA used in [7, 8] is that, first, it allows one to derive the expression for the part of the reaction amplitude having the contribution only from the nearest singularity  $\xi$  in which the influence of the three-body Coulomb dynamics of the transfer mechanism on the peripheral partial amplitudes at  $l_i \gg 1$  is taken into account in a correct manner within the dispersion theory. Second, it accounts for the distortion effects in the initial and final states within the DWBA approach, which is more accurate than as it was done in [18] in the dispersion peripheral model [11]. They allow one to treat the important issue: to what extent does a correct taking into account of the three-body Coulomb effects in the initial, intermediate and final states of the peripheral reaction (1), firstly, influences the spectroscopic information deduced from the analysis of the experimental DCS’s and, secondly, improves the accuracy of the modified DWBA analysis used for obtaining the “experimental” ANC values of astrophysical interest. Besides, the proposed asymptotic theory can also be applied to strong sub-barrier transfer reactions for which the main contribution to the reaction amplitude comes to several lowest partial waves  $l_i$  ( $l_i \sim k_i R_i^{\text{ch}} = 0, 1, \dots$ , where  $k_i \rightarrow 0$  and  $R_i^{\text{ch}} \gtrsim R_N$ ) and the contribution of peripheral partial waves  $l_i$  ( $l_i \gg 1$ ) is strongly suppressed.

The similar theory was proposed earlier in [15] for the peripheral neutron transfer reaction induced by the heavy ions at above-barrier energies, which was also implemented successfully for the specific reactions. However, for peripheral charged particle transfer reactions this task requires a special consideration. This is connected with the considerable complication occurring in the main mechanisms of the reaction (1) because of correct taking into account of the three-body Coulomb dynamics of the transfer mechanism [12, 13].

Below, we use the system of units  $\hbar=c=1$  everywhere, except where they are specially pointed out.

## II. THREE-BODY COULOMB DYNAMICS OF THE TRANSFER MECHANISM AND THE GENERALIZED DWBA

We consider the reaction (1) within the framework of the three ( $A$ ,  $a$  and  $y$ ) charged particles. Within the framework of the three-body Schrödinger approach, the amplitude for the reaction (1) is given by [19, 20]

$$M^{\text{TB}}(E_i, \cos\theta) = \sum_{M_a} \langle \chi_{\mathbf{k}_f}^{(-)} | I_{Aa} V^{\text{TB}} | I_{ay} \chi_{\mathbf{k}_i}^{(+)} \rangle \quad (2)$$

and

$$V^{\text{TB}} = \Delta V_f + \Delta V_f G \Delta V_i. \quad (3)$$

Here  $\chi_{\mathbf{k}_i}^{(+)}$  and  $\chi_{\mathbf{k}_f}^{(-)}$  are the optical Coulomb–nuclear distorted wave functions in the entrance and exit channels with the relative momentum  $\mathbf{k}_i$  and  $\mathbf{k}_f$ , respectively ( $E_i = k_i^2/2\mu_{Ax}$  and  $E_f = k_f^2/2\mu_{By}$ );  $I_{Aa}(\mathbf{r}_{Aa})(I_{ay}(\mathbf{r}_{ay}))$  is the overlap integral of the bound-state  $\psi_A$ ,  $\psi_a$  and  $\psi_B$  ( $\psi_y$ ,  $\psi_a$  and  $\psi_x$ ) wave functions [21, 22];  $\Delta V_f = V_{ay} + V_{yA} - V_f$ ;  $\Delta V_i = V_{Aa} + V_{yA} - V_i$ ;  $G = (\mathcal{E} - H + i \cdot 0)^{-1}$  is the operator of the three-body ( $A$ ,  $a$  and  $y$ ) Green's function and  $M_a$  is the spin projections of the transferred particle  $a$ , where  $V_{ij} = V_{ij}^N + V_{ij}^C$ ,  $V_{ij}^N(V_{ij}^C)$  is the nuclear (Coulomb) interaction potential between the centers of mass of the particles  $i$  and  $j$ , which does not depend on the coordinates of the constituent nucleus;  $V_i$  and  $V_f$  are the optical Coulomb–nuclear potentials in the entrance and exit states, respectively;  $H$  is the Hamiltonian operator for the three-body ( $A$ ,  $a$  and  $y$ ) system;  $\mathcal{E} = E_i - \varepsilon_{ay} = E_f - \varepsilon_{Aa}$  in which  $\varepsilon_{ij}$  is the binding energy of the bound ( $ij$ ) system in respect to the ( $i + j$ ) channel;  $\mathbf{r}_{ij} = \mathbf{r}_i - \mathbf{r}_j$ ,  $\mathbf{r}_i$  is the radius-vector of the center of mass of the particle  $i$  and  $\mu_{ij} = m_i m_j / m_{ij}$  is the reduced mass of the  $i$  and  $j$  particles in which  $m_{ij} = m_i + m_j$  and  $m_j$  is the mass of the  $j$  particle.

The operator of the three-body Green's function  $G$  can be presented as

$$G = G_C + G_C V^N G, \quad G_C = G_0 + G_0 V^C G_C, \quad (4)$$

where  $G_C = (\mathcal{E} - T - V^C + i \cdot 0)^{-1}$  and  $G_0 = (\mathcal{E} - T + i \cdot 0)^{-1}$  are the operators of the three-body ( $A$ ,  $a$  and  $y$ ) Coulomb and free Green's functions, respectively;  $T$  is the kinetic energy operator for the three-body ( $A$ ,  $a$  and  $y$ ) system;  $V^N = V_{ay}^N + V_{Aa}^N + V_{yA}^N$  and  $V^C = V_{ay}^C + V_{Aa}^C + V_{yA}^C$ .

The overlap function  $I_{Aa}(\mathbf{r}_{Aa})$  is given by [9]

$$\begin{aligned} I_{Aa}(\mathbf{r}_{Aa}) &= N_{Aa}^{1/2} \langle \psi_A(\zeta_A) \psi_a(\zeta_a) | \psi_B(\zeta_A, \zeta_a; \mathbf{r}_{Aa}) \rangle \\ &= \sum_{l_B \mu_B j_B \nu_B} C_{j_B \nu_B J_A M_A}^{J_B M_B} C_{l_B \mu_B J_a M_a}^{j_B \nu_B} i^{l_B} Y_{l_B \mu_B}(\hat{\mathbf{r}}_{Aa}) I_{Aa; l_B j_B}(r_{Aa}). \end{aligned} \quad (5)$$

Here  $J_j(M_j)$  is the spin (its projection) of the particle  $j$ ;  $\hat{\mathbf{r}}_{Aa} = \mathbf{r}_{Aa}/r_{Aa}$ ,  $j_B$  and  $\nu_B$  ( $l_B$  and  $\mu_B$ ) are the total (orbital) angular momentum and its projection of the particle  $a$  in the nucleus  $B [= (A + a)]$ , respectively;  $C_{a\alpha b\beta}^{c\gamma}$  is the Clebsch-Gordan coefficient, and  $N_{Aa}$  is the factor taking into account the nucleons' identity [9], which is absorbed in the radial overlap function  $I_{Aa; l_B j_B}(r_{Aa})$  being not normalized to unity [21]. In the matrix element (5), the integration is taken over all the internal relative coordinates  $\zeta_A$  and  $\zeta_a$  for the  $A$  and  $a$  nuclei.

The asymptotic behavior of  $I_{Aa; l_B j_B}(r_{Aa})$  at  $r_{Aa} > r_{Aa}^{(N)}$  is given by the relation

$$I_{Aa; l_B j_B}(r_{Aa}) \simeq C_{Aa; l_B j_B} \frac{W_{-\eta_B; l_B+1/2}(2\kappa_{Aa} r_{Aa})}{r_{Aa}}, \quad (6)$$

where  $W_{\alpha; \beta}(r_{Aa})$  is the Whittaker function,  $\eta_B = z_A z_a e^2 \mu_{Aa} / \kappa_{Aa}$  is the Coulomb parameter for the  $B [= (A + a)]$  bound state,  $\kappa_{Aa} = \sqrt{2\mu_{Aa} \varepsilon_{Aa}}$ ,  $r_{ij}^{(N)}$  is the nuclear interaction radius between  $i$  and  $j$  particles in the bound ( $i + j$ ) state and  $C_{Aa; l_B j_B}$  is the ANC for  $A + a \rightarrow B$ , which is related to the NVC ( $G_{Aa; l_B j_B}$ ) for the virtual decay  $B \rightarrow A + a$  as [9]

$$G_{Aa; l_B j_B} = -i^{l_B + \eta_B} \frac{\sqrt{\pi}}{\mu_{Aa}} C_{Aa; l_B j_B}. \quad (7)$$

Eqs. (5)–(7) and the expression for the matrix element  $M_{Aa}(\mathbf{q}_{Aa})$  for the virtual decay  $B \rightarrow A + a$ , which is given by Eq. (B1) in Appendix B, hold for the matrix element  $M_{ay}(\mathbf{q}_{ay})$  of the virtual decay  $x \rightarrow y + a$  and the overlap function  $I_{ay}(\mathbf{r}_{ay})$ .

The first ( $V_{ay}$ ) and second ( $V_{yA}$ ) terms, entering the first term of the right-hand side (r.h.s.) of (3), correspond to the mechanisms described by the pole and triangle diagrams in Figs. 1a and 1b, respectively, where the Coulomb-nuclear core-core ( $A + y \rightarrow A + y$ ) scattering in the four-ray vertex of the triangle diagram of Fig. 1b is taken in the Born approximation. The  $\Delta V_f G \Delta V_i$  term in the r.h.s. of (3) corresponds to more complex mechanisms than the pole and triangle ones. This term is described by a sum of nine diagrams obtained from the basic diagrams presented in Figs. 1a and 1b, which take into account all possible subsequent mutual Coulomb-nuclear rescattering of the particles  $A$ ,  $a$  and  $y$  in the intermediate state. One of the nine diagrams corresponding to the term  $V_{yA} G V_{Aa}$  is plotted in Fig. 1c, where the Coulomb-nuclear ( $y + A \rightarrow y + A$  and  $A + a \rightarrow A + a$ ) scatterings in the four-ray vertices, including in all four-ray vertices for the others of eight diagrams, are taken in the Born approximation. This term corresponds to the mechanism of subsequent Coulomb-nuclear rescattering of the  $y$  and  $a$  particles, virtually emitted by the projectile  $x$ , on the target  $A$  in the intermediate state. In particular, for the nucleon ( $N$ ) transfer  $A(d, N)B$  reaction, this mechanism corresponds to that of the subsequent scatterings of the proton ( $p$ ) and neutron ( $n$ ), virtually emitted by the deuteron in the field of the  $A$  target, in which the transferred particle is either  $p$  or  $n$ , where  $B = A + N$ .

If the reaction (1) is peripheral, then its dominant mechanism, at least in the angular range of the main peak of the angular distribution, corresponds to the pole diagram in Fig. 1a [11, 15]. The amplitude of this diagram has the singularity at  $\cos \theta = \xi$ , which is the nearest one to the physical ( $-1 \leq \cos \theta \leq 1$ ) region [10, 11] and is given by the expression

$$\xi = \frac{k_{i1}^2 + k_f^2 + \kappa_{ay}^2}{2k_{i1}k_f} = \frac{k_i^2 + k_{f1}^2 + \kappa_{Aa}^2}{2k_i k_{f1}}, \quad (8)$$

where  $k_{i1} = (m_y/m_x)k_i$  and  $k_{f1} = (m_A/m_B)k_f$ . However, if nuclear interactions in the second ( $V_{yA}$ ) and the third ( $V_f$ ) terms of the first  $\Delta V_f$  term of the r.h.s. of (3) as well as in the  $\Delta V_f G \Delta V_i$  one are ignored by the corresponding replacement

$$V_{yA} \rightarrow V_{yA}^C, \quad V_f \rightarrow V_f^C, \quad \Delta V_f G \Delta V_i \rightarrow \Delta V_f^C G_C \Delta V_i^C, \quad (9)$$

where  $\Delta V_f^C = V_{ay}^C + V_{yA}^C - V_f^C$  and  $\Delta V_i^C = V_{Aa}^C + V_{yA}^C - V_i^C$ , then we can separate the part of the amplitude (2), denoted by  $M^{\text{TB}}(E_i, \cos \theta)$  below, which has the singularity at  $\cos \theta = \xi$  (the type of branch point). The remainder of the  $M^{\text{TB}}(E_i, \cos \theta)$  amplitude is given by the sum of an infinite series of the diagrams of the type in Figs. 1b and 1c. They contain all possible nuclear rescattering of the particles  $A$ ,  $a$  and  $y$  from each other in the intermediate state. Therefore, the corresponding amplitudes of these diagrams have singularities ( $\zeta_i$ ), which are located farther away from the left ( $\cos \theta = -1$ ) and right ( $\cos \theta = 1$ ) boundary of the physical ( $-1 \leq \cos \theta \leq 1$ ) region than the singularity  $\xi$  ( $|\zeta_i| > \xi$ ) [10, 23]. Consequently, their contribution to the amplitude  $M^{\text{TB}}(E_i, \cos \theta)$  in the angular range of the main peak of the angular distribution can be ignored [11]. In this approximation, the amplitude

$M^{\text{TB}}(E_i, \cos\theta)$  can be reduced to the form

$$M^{\text{TB}}(E_i, \cos\theta) \approx M^{\text{TBDW}}(E_i, \cos\theta) = M_{\text{post}}^{\text{DW}}(E_i, \cos\theta) + \Delta M^{\text{TBDW}}(E_i, \cos\theta). \quad (10)$$

Here

$$M_{\text{post}}^{\text{DW}}(E_i, \cos\theta) = \sum_{M_a} \langle \chi_{\mathbf{k}_f}^{(-)} I_{Aa} | V_{ay} + V_{yA}^C - V_f^C | I_{ay} \chi_{\mathbf{k}_i}^{(+)} \rangle \quad (11)$$

and

$$\Delta M^{\text{TBDW}}(E_i, \cos\theta) = \sum_{M_a} \langle \chi_{\mathbf{k}_f}^{(-)} I_{Aa} | \Delta V_f^C G_C \Delta V_i^C | I_{ay} \chi_{\mathbf{k}_i}^{(+)} \rangle. \quad (12)$$

In Eqs (10)–(12), the contribution of the three-body ( $A$ ,  $a$  and  $y$ ) Coulomb dynamics of the transfer mechanism in the intermediate state involves all orders of the perturbation theory over the optical Coulomb polarization potentials  $\Delta V_{f,i}^C$ , whereas the Coulomb-nuclear distortions ( $V_i$  and  $V_f$ ) in the entrance and exit channels are taken into account within the framework of the optical model. The amplitude  $M^{\text{TBDW}}(E_i, \cos\theta)$  can be considered as generalization of the post form of the DWBA amplitude ( $M_{\text{post}}^{\text{DW}}(E_i, \cos\theta)$ ) [24] in which the three-body Coulomb dynamics of the main transfer mechanism are taken into account in a correct manner. The pole-approximation of the DWBA amplitude (denoted by  $M_{\text{pole}}^{\text{DW}}(E_i, \cos\theta)$  below) corresponds to the simplest mechanism described by the diagram in Fig. 1a. Its amplitude can be obtained from Eq. (11) if the  $V_{yA}^C - V_f^C$  term in the transition operator is ignored. One notes that the amplitude  $M^{\text{TBDW}}(E_i, \cos\theta)$  passes to the amplitude of the so-called “post”-approximation of the DWBA [20] if all the terms of  $\Delta V_{f,i}^C$  contained in the transition operators of Eqs. (11) and (12) are ignored.

### III. DISPERSION APPROACH AND DWBA

The amplitudes given by Eqs. (11) and (12) defines the behavior both of the amplitude  $M^{\text{TB}}(E_i, \cos\theta)$  at  $\cos\theta = \xi$  [13] and of the corresponding peripheral partial amplitudes at  $l_i \gg 1$  [14]. Besides, owing to the presence of nuclear distortions in the entrance and exit states, these amplitudes have also the singularities located farther from the physical ( $-1 \leq \cos\theta \leq 1$ ) region than  $\xi$ . Therefore, according to [13], the behavior of the  $M_{\text{pole}}^{\text{DW}}(E_i, \cos\theta)$  and  $M_{\text{post}}^{\text{DW}}(E_i, \cos\theta)$  amplitudes near  $\cos\theta = \xi$ , denoted by  $M_{\text{pole}}^{(s)\text{DW}}(E_i, \cos\theta)$  and  $M_{\text{post}}^{(s)\text{DW}}(E_i, \cos\theta)$  below, respectively, can be defined from Eq. (11) as the Coulomb-nuclear distortions in the entrance and exit states are substituted by purely Coulomb ones. The singular  $M_{\text{pole}}^{(s)\text{DW}}(E_i, \cos\theta)$  and  $M_{\text{post}}^{(s)\text{DW}}(E_i, \cos\theta)$  amplitudes near at  $\cos\theta = \xi$  can be presented in the form:

$$M_{\text{pole}}^{\text{DW}}(E_i, \cos\theta) \approx M_{\text{pole}}^{(s)\text{DW}}(E_i, \cos\theta) = N_{\text{pole}}^{\text{DW}} \tilde{M}_{\text{pole}}^{(s)}(E_i, \cos\theta) \quad (13)$$

and

$$M_{\text{post}}^{\text{DW}}(E_i, \cos\theta) \approx M_{\text{post}}^{(s)\text{DW}}(E_i, \cos\theta) = \mathcal{R}_{\text{post}}^{\text{DW}} M_{\text{pole}}^{(s)\text{DW}}(E_i, \cos\theta), \quad (14)$$

$$\mathcal{R}_{\text{post}}^{\text{DW}} = N_{\text{post}}^{\text{DW}}/N_{\text{pole}}^{\text{DW}}, \quad (15)$$

where the explicit forms of  $\tilde{M}_{\text{pole}}^{(s)}(E_i, \cos\theta)$  and of the corresponding peripheral partial amplitudes at  $l_i \gg 1$  ( $\tilde{M}_{l_i; \text{pole}}^{(as)}(E_i)$ ) are given by Eqs. (A1) and (A2) of Appendix A. The peripheral partial amplitudes at  $l_i \gg 1$  corresponding to the  $M_{\text{pole}}^{\text{DW}}(E_i, \cos\theta)$  and  $M_{\text{post}}^{\text{DW}}(E_i, \cos\theta)$  amplitudes are given in Eqs. (A3) and (A4) of Appendix A, respectively. In (15),  $N_{\text{pole}}^{\text{DW}}$  and  $N_{\text{post}}^{\text{DW}}$  are the Coulomb renormalized factors (CRF's) for the  $M_{\text{pole}}^{(s)\text{DW}}(E_i, \cos\theta)$  and  $M_{\text{post}}^{(s)\text{DW}}(E_i, \cos\theta)$  amplitudes, respectively. One notes that the CRF's above are complex numbers and depend on the energy  $E_i$ , the binding energies  $\varepsilon_{ay}$  and  $\varepsilon_{Aa}$  as well as the Coulomb ( $\eta_x, \eta_B, \eta_i$  and  $\eta_f$ ) parameters, where  $\eta_i$  and  $\eta_f$  are the Coulomb parameters in the entrance and exit channels, respectively. Below, for the sake of simplicity of the inscription, in the  $N_{\text{pole}}^{\text{DW}}$  and  $N_{\text{post}}^{\text{DW}}$  the dependences mentioned above will not be pointed out explicitly, except only the dependence on  $E_i$ . This point is also related to the  $N^{\text{TBDM}}$  and  $N^{\text{TBDW}}$  CRF's, which are given by Eq. (18) below and Eq. (A38) in Appendix. The explicit forms of the  $N_{\text{pole}}^{\text{DW}}$  and  $N_{\text{post}}^{\text{DW}}$  CRF's are presented in [13] by the expressions of (14) and (26), respectively, which contain the integrals with the cumbersome integrand. Nevertheless, the approximated analytical forms for the CRF's can be derived and they are presented in Appendix A (see Eqs. (A5) - (A26) there).

The accuracy of the  $M_{\text{post}}^{(s)\text{DW}}(E_i, \cos\theta)$  amplitude can be defined by the extent of proximity of the CRF's  $N_{\text{pole}}^{\text{DW}}$ ,  $N_{\text{post}}^{\text{DW}}$  and  $N^{\text{TBDM}}$  each other. The  $N^{\text{TBDM}}$  CRF determines the power of leading singular term ( $M^{(s)\text{TBDM}}(E_i, \cos\theta)$ ) of the exact (in the model of three ( $A, a$  and  $y$ ) charged particles)  $M^{\text{TBDM}}(E_i, \cos\theta)$  amplitude for the pure sub-barrier peripheral reaction (1) at  $\cos\theta = \xi$ , which has the form [12]

$$M^{\text{TBDM}}(E_i, \cos\theta) \approx M^{(s)\text{TBDM}}(E_i, \cos\theta) = N^{\text{TBDM}} \tilde{M}_{\text{pole}}^{(s)}(E_i, \cos\theta), \quad (16)$$

The explicit form of the CRF  $N^{\text{TBDM}}$  was obtained in [12] by combination of the dispersion method and the three-body Faddeev's equations and is also given by the expressions (A27) - (A31) of Appendix A. Nevertheless, one notes only that the  $M^{(s)\text{TBDM}}(E_i, \cos\theta)$  amplitude includes also all possible subsequent mutual Coulomb rescattering of the  $A, a$  and  $y$  particles in the intermediate state. They are also described by infinite series of diagrams constructed on the basis of the diagrams in Figs. 1a and 1b in which the four-ray vertexes describing the Coulomb  $Aa$ -,  $yA$ - and  $ay$ -rescattering correspond to the total off-shell Coulomb amplitudes [25] but not their Born approximations that used in [13].

As is seen from Eqs. (13), (14) and (16), the  $M_{\text{pole}}^{\text{DW}}(E_i, \cos\theta)$ ,  $M_{\text{post}}^{\text{DW}}(E_i, \cos\theta)$  and  $M^{\text{TBDM}}(E_i, \cos\theta)$  amplitudes near  $\cos\theta = \xi$  behave identically but they differ from each other only by the power. Then, the behavior of the exact three-body  $M^{\text{TB}}(E_i, \cos\theta)$  DWBA amplitude near the singularity at  $\cos\theta = \xi$ , denoted by  $M^{(s)\text{TBDW}}(E_i, \cos\theta)$  below, can be presented in the form as

$$M^{\text{TB}}(E_i, \cos\theta) \approx M^{(s)\text{TBDW}}(E_i, \cos\theta) = \mathcal{R}^{\text{TBDM}} M_{\text{pole}}^{(s)}(E_i, \cos\theta), \quad (17)$$

where

$$\mathcal{R}^{\text{TBDM}}(E_i) = N^{\text{TBDM}}(E_i)/N_{\text{pole}}^{\text{DW}}(E_i). \quad (18)$$

One notes that the expressions (17) and (18) combine the dispersion method in a correct way by taking into account the three-body Coulomb dynamics in the transfer mechanism and the Coulomb distorted effects in the entrance and exit states, as it is done within of the framework of the conventional DWBA. Besides, as is seen from Appendix A, the amplitudes given by Eqs. (14) and (17) can define the peripheral partial amplitudes for  $l_i \gg 1$  of the conventional DWBA and the generalized DWBA, respectively, which differ from each other by their power. Their comparison each other would make it possible to test the accuracy of both the pole-approximation and the post form of the conventional DWBA. Meanwhile, the various relationships are possible between the CRFs  $N_{\text{pole}}^{\text{DW}}$ ,  $N_{\text{post}}^{\text{DW}}$  and  $N^{\text{TBDM}}$  and their ratios  $\mathcal{R}_{\text{post}}^{\text{DW}}$ ,  $\mathcal{R}_{\text{post}}^{\text{TBDW}}$  and  $\mathcal{R}^{\text{TBDM}}$ , where  $\mathcal{R}_{\text{post}}^{\text{TBDW}} = N^{\text{TBDM}}/N_{\text{post}}^{\text{DW}}$ .

However, as is pointed out in [13], in Eqs. (15) and (18) the most “dramatic” situation arises for the calculated CRF’s and their ratios above at the values of the Coulomb parameters  $\eta_x$ ,  $\eta_B$  or their sum  $\eta_{xB}$  ( $\eta_{xB} = \eta_x + \eta_B$ ) near to a natural number. This situation is related the so-called “dramatic” case [13]. In Table 1, as an example related to the “dramatic” case, the results of the calculations of the CRF’s for first two the specific reactions are presented (see the first–eighth lines). Those reactions were considered in Refs. [26, 27, 28] within the framework of the post form of DWBA. In Table 1, for simplicity, the renormalized CRF’s  $\tilde{N}_{\text{pole}}^{\text{DW}} = N_{\text{pole}}^{\text{DW}}/\Gamma$ ,  $\tilde{N}_{\text{post}}^{\text{DW}} = N_{\text{post}}^{\text{DW}}/\Gamma$  and  $\tilde{N}^{\text{TBDM}} = N^{\text{TBDM}}/\Gamma$  are presented since all the CRF’s ( $N_{\text{pole}}^{\text{DW}}$ ,  $N_{\text{post}}^{\text{DW}}$  and  $N^{\text{TBDM}}$ ) contain the common multiplier  $\Gamma (\equiv \Gamma(1 - \eta_{xB} + i\eta_{ij}))$ , where  $\Gamma(\dots)$  is the Euler’s function,  $\eta_{if} = \eta_i + \eta_f$ , and  $\eta_i$  and  $\eta_f$  are the Coulomb parameters for the entrance and exit channels, respectively. Hence, the ratios of the CFR’s presented in the fifth column of Table 1 do not depend on the multiplier  $\Gamma$ . As is seen from Table 1, the values of the  $\tilde{N}_{\text{pole}}^{\text{DW}}$ ,  $\tilde{N}_{\text{post}}^{\text{DW}}$  and  $\tilde{N}^{\text{TBDM}}$  factors calculated in the present work for the peripheral proton transfer  $^{10}\text{B}(^7\text{Be}, ^8\text{B})^9\text{Be}$  [26] and  $^{14}\text{N}(^7\text{Be}, ^8\text{B})^{13}\text{C}$  [27, 28] reactions at the projectile energy of 85 MeV differ significantly from each other. Besides, the calculated values of  $|\mathcal{R}_{\text{post}}^{\text{DW}}| = |\tilde{N}_{\text{post}}^{\text{DW}}/\tilde{N}_{\text{pole}}^{\text{DW}}|$ ,  $|\mathcal{R}_{\text{post}}^{\text{TBDW}}| = |\tilde{N}^{\text{TBDM}}/\tilde{N}_{\text{post}}^{\text{DW}}|$  and  $|\mathcal{R}^{\text{TBDM}}| = |\tilde{N}^{\text{TBDM}}/\tilde{N}_{\text{pole}}^{\text{DW}}|$ , which are also presented in the curly brackets of the last column of Table 1, noticeably differ from each other. One notes that the CRF  $\tilde{N}^{\text{TBDM}}$  determines the power of the peripheral partial amplitudes at  $l_i \gg 1$  of the true three-body  $M^{\text{TBDM}}(E_i, \cos\theta)$  amplitude. Therefore, it is clear that the calculations of the peripheral partial amplitudes at  $l_i \gg 1$ , which are determined by Eq. (A4) and are dominant in the DWBA amplitude of the reactions considered above (at least in the angular range of the main peak of the angular distribution), cannot be performed only with the account the first order of the perturbation theory in  $\Delta V_f^C$  in the amplitude (10). Hence, the expressions (17) and (18) cannot be used for the specific peripheral proton transfer reactions considered above.

A provenance of the main reason of the “dramatic” case is discussed in detail in Appendix A. Nevertheless, we should only note the following fact. In that case, as noted in Appendix A, in the transition operator of the expressions (11) and (12), the poor convergence occurs for a series of the power expansion over  $\Delta V_{i,f}^C$ . It is mainly caused owing to the presence of the vertex Coulomb  $F_C [=F_C(\eta_x, \eta_B)]$  factor as a multiplier in the expressions for the  $\tilde{N}_{\text{pole}}^{\text{DW}}$  and  $\tilde{N}_{\text{post}}^{\text{DW}}$  CRF’s derived within the conventional DWBA (see Appendix A). As is shown in Appendix, the  $F_C$  factor, which is defined by Eq. (A17) of Appendix A, enters implicitly the  $\tilde{N}_{\text{pole}}^{\text{DW}}$  and  $\tilde{N}_{\text{post}}^{\text{DW}}$  CRF’s presented approximately in the forms of Eqs. (A25) and (A25) of

Appendix. In the “dramatic” case, as it is shown by the calculations performed by us, the value of the  $F_C$  factor is not sufficiently close to unity. It happens when the values of the Coulomb parameters  $\eta_x$ ,  $\eta_B$  or their sum ( $\eta_{xB} = \eta_x + \eta_B$ ) being in the vicinity of a natural number [13]. It mainly is one of the main reasons of initiation of this difference observed between the  $\tilde{N}_{\text{pole}}^{\text{DW}}$ ,  $\tilde{N}_{\text{post}}^{\text{DW}}$  and  $\tilde{N}^{\text{TBDW}}$  CRF’s for the peripheral proton transfer reactions [26, 27, 28]. For example, as is seen from Table 1, the calculated values of the vertex Coulomb  $F_C$  factor, are equal to 0.695 ( $\eta_{xB} = 1.823$ ) for the  $^{10}\text{B}(^7\text{Be}, ^8\text{B})^9\text{Be}$  reaction and to 0.366 ( $\eta_{xB} = 1.921$ ) for the  $^{14}\text{N}(^7\text{Be}, ^8\text{B})^{13}\text{C}$  one, i.e., they differ noticeably from unity. Perhaps, that is one of the possible reasons why the ANC value for  $^7\text{Be} + p \rightarrow ^8\text{B}$  recommended in [27, 28] is underestimated as a comparison with that of Refs. [29, 30], which leads in turn to the underestimated astrophysical  $S$  factor for the direct radiative capture  $^7\text{Be}(p, \gamma)^8\text{B}$  reaction at solar energies (see [29, 30]). Therefore, in the “dramatic” case, the next terms ( $\Delta V_f^C G_C \Delta V_i^C$ ) of the transition operator in the series in  $\Delta V_{f,i}^C$  should directly be added to the  $M_{\text{post}}^{\text{DW}}(E_i, \cos\theta)$  (or  $M^{\text{TBDW}}(E_i, \cos\theta)$ ) amplitude defined by Eq. (10). This assertion is suggested by the fact that the “dramatic” case does not occur both for the peripheral neutron transfer reactions considered in Ref. [15], where  $\Delta V_f^C = V_{yA}^C$  and  $F_C=1$  ( $\eta_x=0$  and  $\eta_B=0$ ), and for the  $A(d, n)B$  reaction considered in Ref. [30], where  $\Delta V_f^C=0$  and  $F_C=1$  ( $\eta_x=0$  and  $\eta_B \neq 0$ ). Besides, as shown in [13], the “dramatic” case does not arise for peripheral charged-particle transfer reactions as the values of the vertex Coulomb  $F_C$  factor, calculated at  $\eta_x \neq 0$  and  $\eta_B \neq 0$ , close to 1. The latter occurs when the values of the Coulomb parameters  $\eta_x$ ,  $\eta_B$  or their sum  $\eta_{xB}$  are not in the vicinity of a natural number. This case in [13] is called by the “non-dramatic” case [13]. As is seen from Table 1, the peripheral transfer  $^9\text{Be}(^{10}\text{B}, ^9\text{Be})^{10}\text{B}$ ,  $^{16}\text{O}(^3\text{He}, d)^{17}\text{F}$  and  $^{19}\text{F}(p, \alpha)^{16}\text{O}$  reactions are related to the “non-dramatic” case. Therefore, below those reactions will be considered by us in which the residual  $^{10}\text{B}$  nucleus is formed in the ground ( $E^*=0.0$ ;  $J^\pi=3^+$ ) state, the first ( $E^*=0.718$  MeV;  $J^\pi=1^+$ ), second ( $E^*=1.740$  MeV;  $J^\pi=0^+$ ) and third ( $E^*=2.154$  MeV;  $J^\pi=1^+$ ) excited states (denoted by  $^{10}\text{B}_0$ ,  $^{10}\text{B}_1$ ,  $^{10}\text{B}_2$  and  $^{10}\text{B}_3$ , respectively, below) [8], and the residual  $^{17}\text{F}$  nucleus is formed in the ground ( $0.0$ ;  $J^\pi=\frac{5}{2}^+$ ) and first ( $E^*=0.495$  MeV;  $\frac{1}{2}^+$ ) excited states (denoted by  $^{17}\text{F}_0$  and  $^{17}\text{F}_1$ , respectively, below). While, for the  $^{19}\text{F}(p, \alpha)^{16}\text{O}$  reaction [32-34], the residual nucleus is formed in the ground state.

In the ninth – fifty sixth lines of Table 1, the results of the calculations of the CRF’s and their ratios are presented in Table 1 for the reactions mentioned above. As is seen from Table 1, for the peripheral reactions related to the “non-dramatic” case the values the  $F_C$  factor become sufficiently close to unity and, consequently, the difference between the values of the CRF’s and their ratios mentioned above is significantly less than between those calculated for the “dramatic”  $^{10}\text{B}(^7\text{Be}, ^8\text{B})^9\text{Be}$  and  $^{14}\text{N}(^7\text{Be}, ^8\text{B})^{13}\text{C}$  reactions for which the calculated values of the  $F_C$  factor differ considerably from unity, as noted above. This shows the absolute inapplicability of the “post”-approximation of the conventional DWBA used in [7] for the  $^{16}\text{O}(^3\text{He}, d)^{17}\text{F}$  DWBA analysis.

It follows from here that the expressions (14), (15), (17) and (18) can be used for the peripheral transfer reactions (1), which is related only to the “non-dramatic” case, including the specific peripheral proton and triton reactions listed in Table 1.

For this aim, below we will first show how to obtain the singular part of the pole  $M_{\text{pole}}^{\text{DW}}(E_i, \cos\theta)$  DWBA amplitude corresponding to the one-step pole transfer mechanism, which is described

by the pole diagram of Fig. 1a, by separating the contribution from the nearest singularity  $\xi$  to it. Then, from the expression derived for this amplitude, we obtain the generalized DWBA amplitude valid only for the “non-dramatic” case where the contribution of the three-body ( $A$ ,  $a$  and  $y$ ) Coulomb dynamics of the main transfer mechanism to the peripheral partial amplitudes for  $l_i \gg 1$  are taken into account in a correct manner.

#### IV. DISTORTED-WAVE POLE APPROXIMATION

The pole-approximation of the DWBA amplitude can be obtained from Eq. (11). As a result, it has the form as

$$M_{\text{pole}}^{\text{DW}}(E_i, \cos\theta) = \int d\mathbf{r}_i d\mathbf{r}_f \chi_{\mathbf{k}_f}^{(-)*}(\mathbf{r}_f) I_{Aa}^*(\mathbf{r}_{Aa}) V_{ay}(\mathbf{r}_{ay}) I_{ay}(\mathbf{r}_{ay}) \chi_{\mathbf{k}_i}^{(+)}(\mathbf{r}_i). \quad (19)$$

Here  $\mathbf{r}_i \equiv \mathbf{r}_{xA}$ ,  $\mathbf{r}_f \equiv \mathbf{r}_{yB}$  and

$$\begin{aligned} \mathbf{r}_{ay} &= \bar{a}\mathbf{r}_i - \bar{b}\mathbf{r}_f, \\ \mathbf{r}_{Aa} &= -\bar{c}\mathbf{r}_i + \bar{d}\mathbf{r}_f, \end{aligned} \quad (20)$$

where  $\bar{a} = \mu_{Ax}/m_a$ ,  $\bar{b} = \mu_{Ax}/\mu_{Aa}$ ,  $\bar{c} = \mu_{By}/\mu_{ay}$  and  $\bar{d} = \mu_{By}/m_a$ . To obtain the explicit singular behavior of  $M_{\text{pole}}^{\text{DW}}(E_i, \cos\theta)$  at  $\cos\theta = \xi$ , the integral (19) should be rewritten in the momentum representation making use of Eq. (B1) from Appendix B and the Fourier integrals for the distorted optical wave functions in the entrance and exit channels. It takes the form

$$M_{\text{pole}}^{\text{DW}}(E_i, \cos\theta) = \int \frac{d\mathbf{k}}{(2\pi)^3} \frac{d\mathbf{k}'}{(2\pi)^3} \chi_{\mathbf{k}_f}^{(+)}(\mathbf{k}') \mathcal{M}_{\text{pole}}^{\text{DW}}(\mathbf{k}', \mathbf{k}) \chi_{\mathbf{k}_i}^{(+)}(\mathbf{k}), \quad (21)$$

$$\begin{aligned} \mathcal{M}_{\text{pole}}^{\text{DW}}(\mathbf{k}', \mathbf{k}) &= \sum_{M_a} \langle \mathbf{k}', I_{Aa}(\mathbf{q}_{Aa}) | V_{ay}(\mathbf{q}_{ay}) | I_{ay}(\mathbf{q}_{ay}), \mathbf{k} \rangle \\ &= - \sum_{M_a} \frac{M_{ay}(\mathbf{q}_{ay}) M_{Aa}^*(\mathbf{q}_{Aa})}{\frac{q_{Aa}^2}{2\mu_{Aa}} + \varepsilon_{Aa}} \end{aligned} \quad (22)$$

Here  $\mathcal{M}_{\text{pole}}^{\text{DW}}(\mathbf{k}', \mathbf{k})$  is the off-shell of the Born (pole) amplitude;  $\chi_{\mathbf{k}_i}^{(+)}(\mathbf{k})$  and  $\chi_{\mathbf{k}_i}^{(-)}(\mathbf{k})$  are Fourier components of the distorted wave functions in the entrance and exit channels, respectively;  $I_{ay}(\mathbf{q}_{ay})$  and  $I_{Aa}(\mathbf{q}_{Aa})$  as well as  $V_{ay}(\mathbf{q}_{ay})$  are the same for the overlap functions of the Coulomb-nuclear wave functions for the bound ( $y + a$ ) and ( $A + a$ ) states as well as for the Coulomb-nuclear  $V_{ay}(\mathbf{r}_{ay})$  potential, respectively;  $\mathbf{q}_{ay} = \mathbf{k}_1 - \mathbf{k}'$  and  $\mathbf{q}_{Aa} = -\mathbf{k} + \mathbf{k}'_1$ , where  $\mathbf{k}_1 = (m_y/m_x)\mathbf{k}$  and  $\mathbf{k}'_1 = (m_A/m_B)\mathbf{k}'$ . In Eq. (22),  $M_{ay}(\mathbf{q}_{ay})$  is the vertex matrix element (or so-called the vertex function) for the virtual decay  $x \rightarrow y + a$ . Its explicit form is similar to that for the virtual decay  $B \rightarrow A + a$  given by Eq. (B1) in Appendix B.

Using Eq. (B1) from Appendix B and the corresponding expression for  $M_{ay}(\mathbf{q}_{ay})$ , the  $\mathcal{M}_{\text{pole}}^{\text{DW}}(\mathbf{k}', \mathbf{k})$  amplitude can be presented in the form

$$\mathcal{M}_{\text{pole}}^{\text{DW}}(\mathbf{k}', \mathbf{k}) = \sum_{\alpha_B \alpha_x M_a} C(\alpha_B \alpha_x; (J, M)_{x, A, y, B}; J_a M_a) \tilde{\mathcal{M}}_{\text{pole}; \alpha_B \alpha_x}^{\text{DW}}(\mathbf{k}', \mathbf{k}),$$

$$\tilde{\mathcal{M}}_{\text{pole}; \alpha_B \alpha_x}^{\text{DW}}(\mathbf{k}', \mathbf{k}) = I_{Aa; \alpha_B}^*(\mathbf{q}_{Aa}) W_{ay; \alpha_x}(\mathbf{q}_{ay}). \quad (23)$$

Here

$$C(\alpha_B \alpha_x; (J, M)_{x, A, y, B}; J_a M_a) = C_{j_x \nu_x j_y m_y}^{J_x M_x} C_{l_x \mu_x J_a M_a}^{j_x \nu_x} C_{j_B \nu_B J_A M_A}^{J_B M_B} C_{l_B \nu_B J_a M_a}^{j_B \nu_B}$$

and

$$I_{Aa; \alpha_B}(\mathbf{q}_{Aa}) = -2\mu_{Aa} \frac{W_{Aa; \alpha_B}(\mathbf{q}_{Aa})}{q_{Aa}^2 + \kappa_{Aa}^2}, \quad (24)$$

where  $\alpha_\lambda = (l_\lambda, \mu_\lambda, j_\lambda, \nu_\lambda)$ ;  $\lambda = x, B$ ;  $(J, M)$  is the set of  $J_\lambda$  and  $M_\lambda$  ( $\lambda = x, A, y, B$ ), and

$$\begin{aligned} W_{Aa; \alpha_B}(\mathbf{q}_{Aa}) &= \sqrt{4\pi} G_{Aa; l_B j_B}(q_{Aa}) Y_{l_B \mu_B}(\hat{\mathbf{q}}_{Aa}), \\ W_{ay; \alpha_x}(\mathbf{q}_{ay}) &= \sqrt{4\pi} G_{ay; l_x j_x}(q_{ay}) Y_{l_x \mu_x}(\hat{\mathbf{q}}_{ay}) \end{aligned} \quad (25)$$

are the reduced vertex functions for the virtual decays  $B \rightarrow A + a$  and  $x \rightarrow y + a$ , respectively.

In the presence of the long-range Coulomb interactions between particles of  $A, a$  and  $y$ , the reduced vertex functions can be described by the sum of the nonrelativistic diagrams plotted in Fig. 2. The diagram in Fig. 2b corresponds to the Coulomb part of the vertex function, which has a branch point singularity at  $q_{Aa}^2 + \kappa_{Aa}^2 = 0$  ( $q_{ay}^2 + \kappa_{ay}^2 = 0$ ) and generates the singularity  $\xi$  of the  $M_{\text{pole}}^{\text{DW}}(E_i, \cos\theta)$  amplitude at  $k = k_i$  and  $k' = k_f$ . The sum in Fig. 2c involves more complicated diagrams and this part of the vertex function corresponds to the Coulomb-nuclear vertex function, which is regular at the point  $q_{Aa} = i\kappa_{Aa}$  ( $q_{ay} = i\kappa_{ay}$ ). Then, the vertex functions  $W_{Aa; \alpha_B}(\mathbf{q}_{Aa})$  and  $W_{ay; \alpha_x}(\mathbf{q}_{ay})$  can be presented in the forms [35]

$$\begin{aligned} W_{Aa; \alpha_B}(\mathbf{q}_{Aa}) &= W_{Aa; \alpha_B}^{(\text{C})}(\mathbf{q}_{Aa}) + W_{Aa; \alpha_B}^{(\text{CN})}(\mathbf{q}_{Aa}), \\ W_{ay; \alpha_x}(\mathbf{q}_{ay}) &= W_{ay; \alpha_x}^{(\text{C})}(\mathbf{q}_{ay}) + W_{ay; \alpha_x}^{(\text{CN})}(\mathbf{q}_{ay}). \end{aligned} \quad (26)$$

Here, the  $W_{Aa; \alpha_B}^{(\text{C})}$  and  $W_{Aa; \alpha_B}^{(\text{CN})}$  ( $W_{ay; \alpha_x}^{(\text{C})}$  and  $W_{ay; \alpha_x}^{(\text{CN})}$ ) functions are the pure Coulomb and Coulomb-nuclear parts of the vertex functions, respectively. All terms of the sum in Fig. 2c have dynamic singularities, which are generated by internuclear interactions responsible for the so-called dynamic recoil effects [20, 24]. These singularities are located at the points  $q_{Aa} = i\lambda_i \kappa_i$  and  $q_{ay} = i\bar{\lambda}_i \bar{\kappa}_i$  [23, 36], where  $\lambda_i = m_A/m_{b_i}$ ,  $\kappa_i = \kappa_{b_i c_i} + \kappa_{b_i d_i}$ ,  $\bar{\lambda}_i = m_y/m_{e_i}$  and  $\bar{\kappa}_i = \kappa_{e_i f_i} + \kappa_{e_i g_i}$ . At  $k = k_i$  and  $k' = k_f$ , they generate other singularities  $\xi_i$  and  $\bar{\xi}_i$  of the  $M_{\text{pole}}^{\text{DW}}(E_i, \cos\theta)$  amplitude, which are determined by

$$\xi_i = \frac{(k_i m_{b_i}/m_A)^2 + (k_f m_{b_i}/m_B)^2 + \kappa_i^2}{2k_i k_f m_{b_i}^2/m_A m_B}$$

and

$$\bar{\xi}_i = \frac{(k_i m_{e_i}/m_x)^2 + (k_f m_{e_i}/m_y)^2 + \bar{\kappa}_i^2}{2k_i k_f m_{e_i}^2/m_x m_y}.$$

As a rule, they are located farther from the physical ( $-1 \leq \cos\theta \leq 1$ ) region than  $\xi$  ( $\xi_i > \xi$  and  $\bar{\xi}_i > \xi$ ) [23, 35]. For illustration, the positions of these singularities ( $\xi$ ,  $\xi_i$  and  $\bar{\xi}_i$ ),  $\kappa_i$  and  $\bar{\kappa}_i$  calculated for the specific peripheral reactions are presented in Table 3. There, the

positions of only several singularities  $\xi_i$  ( $\bar{\xi}_i$ ), which are the closest to the singularity  $\xi$ , are presented. As can be seen from Table 3, the singularities  $\xi_i$  and  $\bar{\xi}_i$  are located farther from the physical ( $-1 \leq \cos \theta \leq 1$ ) region than the singularity  $\xi$ . Besides, in the diagram in Fig. 2c, the particle  $d_i(g_i)$  can be the neutral  $\pi^0$  pion meson. In this case, the positions of the singularities are located at the point  $q_{Aa} = i(\kappa_{Aa} + \lambda_{\pi^0}^{-1})$  ( $q_{ay} = i(\kappa_{ay} + \lambda_{\pi^0}^{-1})$ ), where  $\lambda_{\pi^0} = \hbar/m_{\pi^0}c$  is the Compton wave-length of the particle  $\pi^0$  equal to 1.414 fm ( $\lambda_{\pi^0}^{-1} = 0.707 \text{ fm}^{-1}$ ). Therefore, the corresponding singularity  $\xi_i$  ( $\bar{\xi}_i$ ) is also located farther from the physical region on the  $\cos \theta$ -plane than the singularity  $\xi$ .

For the surface reaction (1), the contribution of the interior nuclear range to the  $M_{\text{pole}}^{\text{DW}}(E_i, \cos \theta)$  amplitude, which is generated by the singularities of the  $W_{Aa; \alpha_B}^{(\text{CN})}$  and  $W_{ay; \alpha_x}^{(\text{CN})}$  functions, can be ignored at least in the angular range of the main peak of the angular distribution [11, 15]. Therefore, in Eqs. (23) and (24), the vertex functions given by Eq. (25) can be replaced by their singular behavior of the corresponding Coulomb parts in the vicinity of nearest singularities to the physical points  $q_{ay}^2=0$  and  $q_{Aa}^2=0$  (the branch points). These singularities are located at the points  $q_{ay}^2=-\kappa_{ay}^2$  ( $q_{ay} = i\kappa_{ay}$ ) and  $q_{Aa}^2=-\kappa_{Aa}^2$  ( $q_{Aa} = i\kappa_{Aa}$ ) on the  $q_{ay}^2$ - and  $q_{Aa}^2$ -planes, respectively. In the vicinities of these singularity points, the vertex functions above behave as [35]

$$W_{\beta\gamma; \alpha_x}^{(\text{C})}(\mathbf{q}_{\beta\gamma}) \simeq W_{\beta\gamma; \alpha_x}^{(\text{C}; s)}(\mathbf{q}_{\beta\gamma}) = \sqrt{4\pi}\Gamma(1 - \eta_\alpha) \times \left(\frac{q_{\beta\gamma}}{i\kappa_{\beta\gamma}}\right)^{l_\alpha} \left(\frac{\mathbf{q}_{\beta\gamma}^2 + \kappa_{\beta\gamma}^2}{4i\kappa_{\beta\gamma}^2}\right)^{\eta_\alpha} G_{\beta\gamma; l_{\alpha j_\alpha}}(i\kappa_{\beta\gamma}) Y_{l_\alpha \nu_\alpha}(\hat{\mathbf{q}}_{\beta\gamma}) \quad (27)$$

for  $q_{\beta\gamma} \rightarrow i\kappa_{\beta\gamma}$ , where  $G_{\beta\gamma; l_{\alpha j_\alpha}}(i\kappa_{\beta\gamma}) (\equiv G_{\beta\gamma; l_{\alpha j_\alpha}})$  is the NVC for the virtual decay  $\alpha \rightarrow \beta + \gamma$  ( $\gamma = a$ ;  $\alpha = x$  and  $\beta = y$  for the virtual decay  $x \rightarrow y + a$ , and  $\alpha = B$  and  $\beta = A$  for the virtual decay  $B \rightarrow A + a$ ).

As is seen from Eqs. (23), (24) and (27), the off-shell Born amplitude  $\mathcal{M}_{\text{pole}}^{\text{DW}}(\mathbf{k}', \mathbf{k})$  (23) at  $\mathbf{k} = \mathbf{k}_i$  and  $\mathbf{k}' = \mathbf{k}_f$  has the nearest dynamic singularity at  $\cos \theta = \xi$ . Then, the  $\tilde{\mathcal{M}}_{\text{pole}; \alpha_B \alpha_x}^{\text{DW}}(\mathbf{k}', \mathbf{k})$  amplitude in the approximation (27) takes the form

$$\tilde{\mathcal{M}}_{\text{pole}; \alpha_B \alpha_x}^{\text{DW}}(\mathbf{k}', \mathbf{k}) \approx \tilde{\mathcal{M}}_{\text{pole}; \alpha_B \alpha_x}^{(s); \text{DW}}(\mathbf{k}', \mathbf{k}) = I_{Aa; \alpha_B}^{*(s)}(\mathbf{q}_{Aa}) W_{ay; \alpha_x}^{(s)}(\mathbf{q}_{ay}), \quad (28)$$

where

$$W_{ay; \alpha_x}^{(s)}(\mathbf{q}_{ay}) = \sqrt{4\pi} G_{ay; l_x j_x} \Gamma(1 - \eta_{ay}) \left(\frac{q_{ay}}{i\kappa_{ay}}\right)^{l_x} \left(\frac{q_{ay}^2 + \kappa_{ay}^2}{4i\kappa_{ay}^2}\right)^{\eta_x} Y_{l_x \nu_x}(\hat{\mathbf{q}}_{ay}), \quad (29)$$

$$I_{Aa; \alpha_B}^{*(s)}(\mathbf{q}_{Aa}) = -\sqrt{4\pi} G_{Aa; l_B j_B} \Gamma(1 - \eta_B) \left(\frac{q_{Aa}}{i\kappa_{Aa}}\right)^{l_B} \left(\frac{q_{Aa}^2 + \kappa_{Aa}^2}{4i\kappa_{Aa}^2}\right)^{\eta_B} \times \frac{2\mu_{Aa}}{q_{Aa}^2 + \kappa_{Aa}^2} Y_{l_B \nu_B}^*(\hat{\mathbf{q}}_{Aa}). \quad (30)$$

The vertex formfactors  $G_{Aa; l_B j_B}(q_{Aa})$  and  $G_{ay; l_x j_x}(q_{ay})$ , defined from by the expressions (25), (28)–(30), have the kinematic singularities (branch points) for odd-values of the quantum numbers  $l_B$  and  $l_x$  [11]. They arise due to their behaviors as  $G_{Aa; l_B j_B}(q_{Aa}) \propto q_{Aa}^{l_B}$  at  $q_{Aa} \rightarrow 0$  and  $G_{ay; l_x j_x}(q_{ay}) \propto q_{ay}^{l_x}$  at  $q_{ay} \rightarrow 0$ . Nevertheless, as is seen from Eq. (26) as well as from

Eqs. (B3) and (B4) of Appendix B rewritten over the  $\mathbf{q}_{ay}$  and  $\mathbf{q}_{Aa}$  variables, the  $W_{Aa; \alpha_B}(\mathbf{q}_{Aa})$  ( $I_{Aa; \alpha_B}(\mathbf{q}_{Aa})$ ) and  $W_{ay; \alpha_x}(\mathbf{q}_{ay})$  functions as well as the  $\mathcal{M}_{\text{pole}; \alpha_B \alpha_x}^{\text{DW}}(\mathbf{k}', \mathbf{k})$  amplitude do not have these singularities.

Taking into account Eqs. (28) – (30), we now rewrite the integral (21) in the coordinate representation. First, we consider this presentation for the Fourier components of the  $W_{ay; \alpha_x}^{(s)}(\mathbf{q}_{ay})$  and  $I_{Aa; \alpha_B}^{*(s)}(\mathbf{q}_{Aa})$  functions:

$$W_{x; \alpha_x}^{(as)}(\mathbf{r}_{ay}) = \int \frac{d\mathbf{q}_{ay}}{(2\pi)^3} e^{i\mathbf{r}_{ay}\mathbf{q}_{ay}} W_{x; \alpha_x}^{(s)}(\mathbf{q}_{ay}) \quad (31)$$

and

$$I_{B; \alpha_B}^{(as)}(\mathbf{r}_{Aa}) = \int \frac{d\mathbf{q}_{Aa}}{(2\pi)^3} e^{i\mathbf{r}_{Aa}\mathbf{q}_{Aa}} I_{Aa; \alpha_B}^{(s)}(\mathbf{q}_{Aa}) \quad (32)$$

Substituting Eq. (29) in Eq. (31) and Eq. (30) in Eq. (32), the integration over the angular variables can easily be performed making use of the expansion

$$e^{i\mathbf{q}\mathbf{r}} = 4\pi \sum_{l\nu} i^l j_l(qr) Y_{l\nu}^*(\hat{\mathbf{q}}) Y_{l\nu}(\hat{\mathbf{r}}),$$

where  $j_l(z)$  is a spherical Bessel function [37]. The remaining integrals in  $q_{ay}$  and  $q_{Aa}$  can be done by using formula 6.565(4) and Eq. (91) from Refs. [38] and [9], respectively. As a result, one obtains

$$W_{ay; \alpha_x}^{(as)}(\mathbf{r}_{ay}) = -\frac{\sqrt{2}\eta_x}{\pi} G_{ay; l_x j_x} \left( \frac{\kappa_{ay}}{r_{ay}} \right)^{3/2} \frac{K_{l_x+3/2+\eta_x}(\kappa_{ay}r_{ay})}{(2i\kappa_{ay}r_{ay})^{\eta_x}} i^{-l_x} Y_{l_x \nu_x}(\hat{\mathbf{r}}_{ay}) \quad (33)$$

for  $r_{ay} \gtrsim R_x$  and

$$I_{Aa; \alpha_B}^{*(as)}(\mathbf{r}_{Aa}) = -\frac{\sqrt{2}}{\pi} G_{Aa; l_B j_B} \left( \frac{\mu_{Aa}^2 \kappa_{Aa}}{r_{Aa}} \right)^{1/2} \frac{K_{l_B+1/2+\eta_B}(\kappa_{Aa}r_{Aa})}{(2i\kappa_{Aa}r_{Aa})^{\eta_B}} i^{-l_B} Y_{l_B \nu_B}^*(\hat{\mathbf{r}}_{Aa}) \quad (34)$$

for  $r_{Aa} \gtrsim R_B$ . Here  $K_{\bar{\nu}}(z)$  is a modified Hankel function [37] and  $R_C = r_0 C^{1/3}$  is the radius of  $C$  nucleus, where  $C$  is a mass number of the  $C$  nucleus. Using formula 9.235 (2) from [38] and the relation (7), the leading asymptotic terms of Eqs. (33) and (34) can be reduced to the forms

$$W_{ay; \alpha_x}^{(as)}(\mathbf{r}_{ay}) \approx V_{ay}^C(r_{ay}) I_{ay; \alpha_x}^{(as)}(r_{ay}) Y_{l_x \nu_x}(\hat{\mathbf{r}}_{ay}), \quad (35)$$

for  $r_{ay} \gtrsim R_x$  and

$$I_{Aa; \alpha_B}^{*(as)}(\mathbf{r}_{Aa}) \approx C_{l_B j_B} \frac{\exp\{-\kappa_{Aa}r_{Aa} - \eta_B \ln(2\kappa_{Aa}r_{Aa})\}}{r_{Aa}} Y_{l_B \nu_B}^*(\hat{\mathbf{r}}_{Aa}), \quad (36)$$

for  $r_{Aa} \gtrsim R_B$ . In Eq. (35),  $V_{ay}^C(r_{ay}) = Z_a Z_y e^2 / r_{ay}$  is the Coulomb interaction potential between the centers of mass of particles  $y$  and  $a$ , and

$$I_{ay; \alpha_x}^{(as)}(r_{ay}) = C_{l_x j_x} \frac{\exp\{-\kappa_{ay}r_{ay} - \eta_x \ln(2\kappa_{ay}r_{ay})\}}{r_{ay}}, \quad (37)$$

which coincides with the leading term of the asymptotic behavior of the radial component of the overlap function  $I_{ay}(\mathbf{r}_{ay}) \approx I_{ay;\alpha_x}^{(as)}(r_{ay})Y_{l_x\nu_x}(\hat{\mathbf{r}}_{ay})$  for  $r_{ay} > R_x$ .

Following by [36], it can show that the leading terms of the asymptotic expressions for the radial components of the Coulomb-nuclear parts of the  $W_{ay}(\mathbf{r}_{ay})$  and  $I_{Aa}(\mathbf{r}_{Aa})$  functions, which are generated by the singularities of  $\xi_i$  and  $\bar{\xi}_i$  of the  $W_{ay;\alpha_x}^{(CN)}(\mathbf{q}_{ay})$  and  $W_{Aa;\alpha_B}^{(CN)}(\mathbf{q}_{Aa})$  functions, respectively, behave as

$$W_{l_x j_x}^{(CN)}(r_{ay}) \approx \sum_i W_{l_x j_x; i}^{(CN; as)}(r_{ay}), \quad I_{l_B j_B}^{(CN)}(r_{Aa}) \approx \sum_i I_{l_B j_B; i}^{(CN; as)}(r_{Aa}). \quad (38)$$

Here

$$W_{l_x j_x; i}^{(CN; as)}(r_{ay}) = \bar{C}_{l_x j_x}^{(i)} \frac{\exp\{-[\bar{\kappa}_i r_{ay} + \eta_{e_i f_i} \ln(2\bar{\lambda}_i \kappa_{e_i f_i} r_{ay}) + \eta_{e_i g_i} \ln(2\bar{\lambda}_i \kappa_{e_i g_i} r_{ay})]\}}{r_{ay}^2}, \quad (39)$$

$$I_{l_B j_B; i}^{(CN; as)}(r_{Aa}) = C_{l_B j_B}^{(i)} \frac{\exp\{-[\kappa_i r_{Aa} + \eta_{b_i c_i} \ln(2\lambda_i \kappa_{b_i c_i} r_{Aa}) + \eta_{b_i d_i} \ln(2\lambda_i \kappa_{b_i d_i} r_{Aa})]\}}{r_{Aa}^2}, \quad (40)$$

where  $\eta_{\alpha\beta}$  is the Coulomb parameter for the bound  $(\alpha + \beta)$  system in the tri-ray vertex of the diagram in Fig. 2c. Explicit expressions for  $\bar{C}_{l_x j_x}^{(i)}$  and  $C_{l_B j_B}^{(i)}$  can be obtained from Eqs. (B.4) and (B.5) of [36], which are expressed in the terms of the product of the corresponding ANC's for the tri-rays vertices of the diagrams in Fig. 2c. As is seen from Eqs. (38) – (40), if  $\kappa_i > \kappa_{Aa}$  and  $\bar{\kappa}_i > \kappa_{ya}$ , then the asymptotic terms given by the expressions (39) and (40) decrease more rapidly with increasing  $r_{ay}$  and  $r_{Aa}$ , respectively, than those of (35) and (36). See Table 3, where  $\kappa_i > \kappa_{Aa}$  and  $\bar{\kappa}_i > \kappa_{ya}$  for all the considered reactions. Therefore, the use of the pole approximation is reasonable in calculations of the leading terms of the peripheral partial wave amplitudes at  $l_i \gg 1$  determined correctly by only the nearest singularity  $\xi$ , which is in turn equivalent to the replacements of  $V_{ay}(\mathbf{r}_{ay})I_{ay}(\mathbf{r}_{ay})$  and  $I_{Aa;\alpha_B}^*(\mathbf{r}_{Aa})$  by  $W_{ay;\alpha_x}^{(as)}(\mathbf{r}_{ay})$  and  $I_{Aa;\alpha_B}^{*(as)}(\mathbf{r}_{Aa})$  in the integrand function of Eq. (19), respectively. These peripheral partial wave amplitudes indeed give the dominant contribution to the  $M_{\text{pole}}^{\text{DW}}(E_i, \cos\theta)$  at least in the angular range of the main peak of the angular distribution [11].

In this case, the  $M_{\text{pole}}^{\text{DW}}(E_i, \cos\theta)$  amplitude in the coordinate representation can be reduced to the form as

$$M_{\text{pole}}^{\text{DW}}(E_i, \cos\theta) \simeq M_{\text{pole}}^{(s)\text{DW}}(E_i, \cos\theta) = \sum_{\alpha_B \alpha_x M_a} C(\alpha_B \alpha_x; (J, M)_{x, A, y, B}; J_a M_a) \times \tilde{M}_{\text{pole}; \alpha_B \alpha_x}^{\text{DW}}(E_i, \cos\theta), \quad (41)$$

where

$$\tilde{M}_{\text{pole}; \alpha_B \alpha_x}^{\text{DW}}(E_i, \cos\theta) = \int d\mathbf{r}_i d\mathbf{r}_f \Psi_{\mathbf{k}_f}^{*(-)}(\mathbf{r}_f) I_{Aa;\alpha}^{*(as)}(\mathbf{r}_{Aa}) W_{ay;\alpha_x}^{(as)}(\mathbf{r}_{ay}) \Psi_{\mathbf{k}_i}^{(+)}(\mathbf{r}_i). \quad (42)$$

One notes that the expressions for  $W_{ay;\alpha_x}^{(as)}(\mathbf{r}_{ay})$ , given by Eqs. (33) and (35), is valid for  $\eta_x > 0$ . For  $\eta_x=0$ , the Fourier component of the  $W_{x;\alpha_x}^{(as)}(\mathbf{r}_{ay})$  function in (31) is given only by

the kinematic function  $q_{ay}^{l_x}$  for  $l_x > 0$  and, so, the Fourier integral becomes singular [15]. In this case, for  $\eta_x = 0$  one obtains

$$W_{ay;\alpha_x}^{(as)}(\mathbf{r}_{ay}) = -\frac{C_{l_x j_x} \hat{l}_x!! (\kappa_{ay} r_{ay})^{-l_x} \delta(r_{ay}) r_{ay}^{-2} Y_{l_x \nu_x}(\hat{\mathbf{r}}_{ay})}{2\mu_{ay}}, \quad (43)$$

where  $r_{ay}$  is given by Eq. (20) and  $\hat{l}_x = 2l_x + 1$ . This expression corresponds to the vertex function for the virtual decay  $x \rightarrow y + a$  [15] calculated in the well-known zero-range approximation. Therefore, the expression (43) can be applied jointly with Eq. (34) for the  $M_{\text{pole}}^{\text{DW}}(E_i, \cos\theta)$  amplitude of the peripheral  $A(d, n)B$  reaction for example.

We now expand the  $M_{\text{post};\text{pole}}^{\text{DW}}(E_i, \cos\theta)$  amplitude in partial waves. To this end, in (42) we use the partial-waves expansions (B3) and (B4) from Appendix B and the expansion

$$\begin{aligned} & \frac{K_{l_{ay}+3/2+\eta_x}(\kappa_{ay} r_{ay})}{r_{ay}^{l_{ay}+\eta_x+3/2}} \frac{K_{l_{Aa}+1/2+\eta_B}(\kappa_{Aa} r_{Aa})}{r_{Aa}^{l_{Aa}+\eta_B+1/2}} \\ &= 4\pi \sum_{l\mu_i} \mathcal{A}_l(r_i, r_f) Y_{l\mu_i}(\hat{\mathbf{r}}_i) Y_{l\mu_i}^*(\hat{\mathbf{r}}_f). \end{aligned} \quad (44)$$

Here

$$\mathcal{A}_l(r_i, r_f) = \frac{1}{2} \int_{-1}^1 \frac{K_{l_{ay}+3/2+\eta_x}(\kappa_{ay} r_{ay})}{r_{ay}^{l_{ay}+\eta_x+3/2}} \frac{K_{l_{Aa}+1/2+\eta_B}(\kappa_{Aa} r_{Aa})}{r_{Aa}^{l_{Aa}+\eta_B+1/2}} P_l(z) dz, \quad (45)$$

where  $r_{ay} = [(\bar{a}r_i)^2 + (\bar{b}r_f)^2 - 2\bar{a}\bar{b}r_i r_f z]^{1/2}$ ,  $r_{Aa} = [(\bar{c}r_i)^2 + (\bar{d}r_f)^2 - 2\bar{c}\bar{d}r_i r_f z]^{1/2}$  and  $z = (\hat{\mathbf{r}}_i \hat{\mathbf{r}}_f)$ . The integration over the angular variables  $\hat{\mathbf{r}}_i$  and  $\hat{\mathbf{r}}_f$  in Eq. (42) can easily be done by using Eqs. (B5) and (B6) of Appendix B. After some simple, but cumbersome algebra using the corresponding formulae from [39], one finds that the pole amplitude  $M_{\text{pole}}^{\text{DW}}(E_i, \cos\theta)$  in the system  $z \parallel \mathbf{k}_i$  has the form

$$\begin{aligned} M_{\text{pole}}^{\text{DW}}(E_i, \cos\theta) &= -8\sqrt{\frac{2}{\pi}} \frac{1}{\mu_{ay}} \frac{1}{k_i k_f} \sum_{j_x \tau_x} \sum_{j_B \tau_B} \sum_{JM} \sum_{l_x l_B} (-1)^{j_B - J_a + J} i^{l_x + l_B} (\hat{l}_x \hat{l}_B) (\hat{J} \hat{j}_B)^{1/2} \\ &\times C_{ay; l_x j_x} C_{Aa; l_B j_B} C_{j_B \tau_B J_A M_A}^{J_B M_B} C_{j_x \tau_x J_y M_y}^{J_x M_x} C_{JM j_B \tau_B}^{J_x \tau_x} W(l_x j_x l_B j_B; J_a J) \\ &\times \sum_{l_i l_f} M_{l_x l_B J l_i l_f}^{\text{pole}}(E_i) C_{l_i 0 l_f M}^{J M} Y_{l_f M}(\theta, 0) \end{aligned} \quad (46)$$

where the explicit form of  $M_{l_x l_B J l_i l_f}^{\text{pole}}(E_i)$  is given by Eqs. (B7) – (B10) of Appendix B.

It should be noted that just neglecting the dynamic recoil effect mentioned above, which is caused by using the pole approximation in the matrix elements for the virtual decays  $x \rightarrow y + a$  and  $B \rightarrow A + a$ , results in the fact that the radial integral (B8) of the  $M_{\text{pole}}^{\text{DW}}(E_i, \cos\theta)$  amplitude, given in Appendix B, does not contain the  $V_{ya}$  and  $V_{Aa}$  potentials in contrast to that of the conventional DWBA with recoil effects [20, 24]. That is the reason why the  $M_{\text{pole}}^{\text{DW}}(E_i, \cos\theta)$  amplitude is parametrized directly in the terms of the ANCs (or respective the NVCs) but not in those of the spectroscopic factors, as it occurs for the conventional DWBA [20, 24].

## V. THREE-PARTICLE COULOMB DYNAMICS OF THE TRANSFER MECHANISM AND THE GENERALIZED DWBA

We now consider how to take into account accurately the contribution of the three-body Coulomb dynamics of the transfer mechanism to the  $M_{\text{pole}}^{\text{DW}}(E_i, \cos\theta)$  and  $M^{\text{TBDW}}(E_i, \cos\theta)$  amplitudes by using Eqs. (17), (18) and (46) as well as Eqs. (B7) and (B8) from Appendix B. To this end, we should compare their partial wave amplitudes for  $l_i \gg 1$  and  $l_f \gg 1$  (denoted by  $M_{l_i l_f}^{\text{TBDW}}(E_i)$  and  $M_{\text{pole}; l_i l_f}^{\text{DW}}$  below) with each other, which can be determined from the corresponding expressions for the  $M^{(s)\text{TBDW}}(E_i, \cos\theta)$  and  $M_{\text{pole}}^{(s)\text{DW}}(E_i, \cos\theta)$  amplitudes.

According to [14], from Eq. (17) and (18), the peripheral partial amplitudes at  $l_i \gg 1$  and  $l_f \gg 1$  can be presented in the form as

$$M_{l_i l_f}^{\text{TBDW}}(E_i) = \mathcal{R}^{\text{TBDM}}(E_i) M_{\text{pole}; l_i l_f}^{\text{DW}}(E_i). \quad (47)$$

Here  $M_{\text{pole}; l_i l_f}^{\text{DW}}(E_i)$  is the peripheral partial amplitude corresponding to the pole approximation of the DWBA amplitude.

The expression (47) can be considered as the peripheral partial amplitude of the generalized DWBA in which the contribution of the three-body Coulomb dynamics of the main transfer mechanism is correctly taken into account. For  $l_i \gg 1$  and  $l_f \gg 1$  the asymptotics of the pole approximation ( $M_{\text{pole}; l_i l_f}^{\text{DW}}(E_i)$ ) partial amplitudes of the pole-approximation DWBA amplitude and the exact three-body ( $M_{l_i l_f}^{\text{TBDW}}(E_i)$ ) partial amplitudes of the exact three-body amplitude have the same dependence on  $l_i$  and  $l_f$ . Nevertheless, they differ only in their powers.

Therefore, if the main contribution to the  $M^{\text{TBDW}}(E_i, \cos\theta)$  amplitude comes from the peripheral partial waves with  $l_i \gg 1$  and  $l_f \gg 1$ , then the expression (47) makes it possible to obtain the amplitude of the generated three-body DWBA. For this aim, in Eq. (46) the expression  $M_{l_x l_B J l_i l_f}^{\text{pole}}(E_i)$  at fixed values  $l_x$ ,  $l_B$  and  $J$  has to be renormalized by the replacement

$$M_{l_x l_B J l_i l_f}^{\text{pole}}(E_i) \longrightarrow M_{l_x l_B J l_i l_f}^{\text{TBDW}}(E_i) = \mathcal{N}_{l_i l_f}^{\text{TBDM}}(E_i) M_{l_x l_B J l_i l_f}^{\text{pole}}(E_i). \quad (48)$$

Here

$$\mathcal{N}_{l_i l_f}^{\text{TBDM}}(E_i) = \begin{cases} 1, & \text{for } l_i < L_0 \text{ and } l_f < L_0; \\ \mathcal{R}^{\text{TBDM}}(E_i) & \text{for } l_i \geq L_0, l_f \geq L_0, \end{cases} \quad (49)$$

where  $L_0 \sim k_i R_i^{\text{ch}}$  (or  $\sim k_f R_f^{\text{ch}}$ ). In this case, the expression for the amplitude of the generalized three-body DWBA,  $M^{\text{TBDW}}(E_i, \cos\theta)$ , is given by

$$\begin{aligned} M^{\text{TB}}(E_i, \cos\theta) &\approx M^{(s)\text{TBDW}}(E_i, \cos\theta) = -8 \sqrt{\frac{2}{\pi}} \frac{1}{\mu_{ay}} \frac{1}{k_i k_f} \sum_{j_x \tau_x j_B \tau_B} \sum_{J, M} \sum_{l_x l_B} \\ &\times C_{ay; l_x j_x} C_{Aa; l_B j_B} C_{j_B \tau_B J_A M_A}^{J_B M_B} C_{j_x \tau_x j_y M_y}^{J_x M_x} C_{J M j_B \tau_B}^{j_x \tau_x} \sum_{l_i l_f} M_{l_x l_B J l_i l_f}^{\text{TBDW}}(E_i) C_{l_i 0 l_f M}^{J M} Y_{l_f M}(\theta, 0), \end{aligned} \quad (50)$$

where the expression for  $M_{l_x l_B J l_i l_f}^{\text{TBDW}}(E_i)$  is obtained from Eq. (B7) of Appendix B by the substitution of the  $M_{l_x l_B J l_i l_f}^{\text{pole}}(E_i)$  by  $M_{l_x l_B J l_i l_f}^{\text{TBDW}}(E_i)$  defined by Eq. (48). The expression (50) can be

considered as a generalization of Eqs. (34) and (35) of Ref. [15] derived within the framework of the dispersion theory for the above-barrier peripheral neutron transfer reaction. As is seen from Eqs. (48) – (50) as well as from Eqs. (B7) and (B8) of Appendix B, in Eq. (50), the contribution of non-peripheral partial waves to the generalized three-body DWBA amplitude is taken into account in the pole-approximation.

From Eqs. (46), (48) and (49), we can now derive the expression for the differential cross section for the generalized three-body DWBA, which has the form as

$$\begin{aligned} \frac{d\sigma}{d\Omega} = & \frac{\mu_{Ax}\mu_{By}k_f}{(2\pi^2)^2} \frac{1}{k_i \hat{J}_A \hat{J}_x} \sum_{M_A M_x M_B M_y} |M^{(s)\text{TBDW}}(E_i, \cos\theta)|^2 = \frac{20(\hbar c)^2}{\pi^3 E_i E_f} \left(\frac{\hbar}{\mu_{ay}c}\right)^2 \frac{k_f \hat{J}_B}{k_i \hat{J}_A} \\ & \times \sum_{j_x j_B} \sum_{JM} | \sum_{l_x l_B} \sum_{l_i l_f} \exp\{i[\sigma_{l_i} + \sigma_{l_f} + \frac{\pi}{2}(l_i + l_f + l_x + l_B)]\} C_{ay;l_x j_x} C_{Aa;l_B j_B} \\ & \times (\hat{l}_x \hat{l}_B) (\hat{l}_i^2 \hat{l}_f)^{1/2} W(l_x j_x l_B j_B; J_a J) C_{l_i 0 l_f M}^{JM} M_{l_x l_B J l_i l_f}^{\text{TBDW}}(E_i) Y_{l_f M}(\theta, 0) |^2. \end{aligned} \quad (51)$$

Herein, the ANCs  $C$ 's,  $\kappa_{ij}(k_i$  and  $k_f)$  and  $d\sigma/d\Omega$  are in  $\text{fm}^{-1/2}$ ,  $\text{fm}^{-1}$  and  $\text{mb}/\text{sr}$ , respectively, and  $E_i$  and  $E_f$  are in MeV. One notes that Eq. (51) and Eq. (B8) given in Appendix B contain the cut-off parameters  $R_i^{\text{ch}}$  and  $R_f^{\text{ch}}$ , which are determined by only the free parameter  $r_0$  (see Appendix B).

The expression (51) can also be applied for peripheral sub-barrier charged particle transfer reactions for which the dominant contribution comes to rather low partial waves with  $l_i \sim k_i R_i^{\text{ch}} \sim 0, 1, \dots$ , which correspond to  $k_i \rightarrow 0$  and  $R_i^{\text{ch}} \gtrsim R_N$ . Here, it is assumed that the contribution of the low partial amplitudes to the reaction amplitude parametrizing via the product of the ANCs (or NVCs) for  $R_i^{\text{ch}} \gtrsim R_N$  can be taken into account in the pole-approximation of the DWBA. In this case, the contribution of the peripheral partial waves with  $l_i \gg 1$  and  $l_f \gg 1$  to the reaction amplitude is strongly suppressed as  $\tau \gg 1$  in Eqs. (A2) – (A4) (see Section IV below). Nevertheless, the influence of the three-body Coulomb dynamics of the transfer mechanism on the DCS (51) is mainly taken into account via the interference term between the low and peripheral partial amplitudes arising from Eqs. (48) and (49). In this connection, one notes that the analogous situation occurs for the peripheral direct nuclear-astrophysical  $A(a, \gamma)B$  reaction at extremely low (sub-barrier) energies for which the radiative capture proceeds also at the large relative distances of the colliding particles  $r_{Aa} \gtrsim R_N$ . For this reaction the main contribution in the long-wavelength approximation comes to the partial waves with  $l_i \sim 0, 1, \dots$ , and the reaction amplitude can also be expressed in the term of the ANC for  $A + a \rightarrow B$  [5, 29].

## VI. RESULTS OF THE ANALYSIS OF THE PERIPHERAL PARTIAL AMPLITUDES FOR THE SPECIFIC SUB- AND ABOVE-BARRIER REACTIONS

In this section, we present the results of calculations of the modulus of the partial amplitudes  $|M_{l_x l_B J l_i l_f}^{\text{TBDW}}|$  (denoted by  $|M_{J l_i l_f}|$  for the fixed values of the angular momenta  $l_x$  and  $l_B$

below) of the amplitude (50). The calculation were performed for the following peripheral proton and triton transfer reactions:

(I)  ${}^9\text{Be}({}^{10}\text{B}, {}^9\text{Be}){}^{10}\text{B}_i$  ( $i=0-3$ ) at the  ${}^{10}\text{B}$  incident energy  $E_{10\text{B}}=100$  MeV [8];

(II)  ${}^{16}\text{O}({}^3\text{He}, d){}^{17}\text{F}_i$  ( $i=0$  and  $1$ ) at  $E_{3\text{He}}=29.75$  MeV [31];

(III)  ${}^{19}\text{F}(p, \alpha){}^{16}\text{O}(\text{g.s.})$  at six sub-barrier proton projectile energie of  $E_p=250, 350$  and  $450$  MeV [32, 33] and  $E_p=327, 387$  and  $486$  MeV [34].

One notes once more that all they are related to the “non-dramatic” case (see the first column of Table 1).

For the reactions considered above, the orbital ( $l_B$  and  $l_x$ ) angular momentums of the transfer (proton or triton) particle are taken equal to  $l_{10\text{B}_i}=1$  ( $i=0-3$ ),  $l_{17\text{F}_0}=2$  and  $l_{17\text{F}_1}=0$ , and  $l_{3\text{He}}=l_\alpha=0$ . Since the energy of incident  ${}^3\text{He}$  in the reaction (II) is moderate, the contribution of the  $D$ -state of the  ${}^3\text{He}$  nucleus in the vertex  ${}^3\text{He} \rightarrow d + p$  is neglectable small [9]. Calculations were performed the optical potentials in the initial and final states, which were taken from Refs. [8, 31] (the sets 1 and 2) and [33] for the standard values of the parameter  $r_0$  ( $r_0=1.25$  fm).

In order to estimate the influence of the three-body Coulomb dynamics of the transfer mechanism on the peripheral partial amplitudes at  $l_i \gg 1$  and  $l_f \gg 1$ , we have analyzed only the contribution of the different partial wave amplitudes to the amplitude (50). Fig. 3 shows the  $l_i$  dependence of the modulus of the partial amplitudes ( $|M_{Jl_i l_f}|$ ) for the fixed values of  $l_x$  and  $l_B$  above. As is seen from Fig. 3a, the contribution to the amplitude of the  ${}^9\text{Be}({}^{10}\text{B}, {}^9\text{Be}){}^{10}\text{B}_0$  reaction from lower partial amplitudes with  $l_i < 14$  is strongly suppressed due to the strong absorption in the entrance and exit channels. Nevertheless, for the transferred angular momentum  $J=0$  the contributions of the three-body Coulomb effects to the peripheral partial  $|M_{Jl_i l_f}|$  amplitudes change from 55% to 7% for the  ${}^9\text{Be}({}^{10}\text{B}, {}^9\text{Be}){}^{10}\text{B}_0$  reaction at  $l_i \geq 16$  (see the inset in Fig. 3). It should be noted that the orbital angular momenta  $l_i$  for this reaction are  $l_i \sim k_i R_i^{\text{ch}} \approx 16$  for the channel radius  $R_i^{\text{ch}} \approx 5.3$ . The same situation occurs for the reaction populating the excited states of  ${}^{10}\text{B}_i$  ( $i=1-3$ ) mentioned above. Besides, the analogous contribution is found to be about 20–30 for the  ${}^{16}\text{O}({}^3\text{He}, d){}^{17}\text{F}_0$  reaction for which  $l_i \sim k_i R_i^{\text{ch}} \approx 8$  for the channel radius  $R_i^{\text{ch}} \approx 5$  fm (see the inset in Fig. 3b). For the  ${}^{16}\text{O}({}^3\text{He}, d){}^{17}\text{F}_1$  reaction the influence of the three-body Coulomb effects on the peripheral partial amplitudes is extremely larger as compared with that for the  ${}^{16}\text{O}({}^3\text{He}, d){}^{17}\text{F}_0$  reaction (see Table reftable1). For example, the ratio of the partial  $|M_{Jl_i l_f}|$  amplitudes, calculated with taking into account of the Coulomb renormalized  $\mathcal{N}_{l_i l_f}^{\text{TBDM}}(E_i)$  factor (see Eqs. (48) and (49)) to that calculated without taking into account of this factor ( $\mathcal{N}_{l_i l_f}^{\text{TBDM}}(E_i)=1$ ) in the peripheral partial amplitudes, changes about from  $1.3 \times 10^{-7}$  to  $2.2 \times 10^{-7}$  for  $l_i \geq 13$ . This is the result of the significant difference between the ratio  $R^{\text{TBDM}}$  calculated for the ground and first excited states of the residual  ${}^{17}\text{F}$  nucleus (see Table 1). In Fig. 3c, as an illustration, the same  $l_i$  dependence is displayed for the sub-barrier  ${}^{19}\text{F}(p, \alpha){}^{16}\text{O}$  reaction at the energy  $E_p=0.250$  MeV for which  $l_i \sim k_i R_i^{\text{ch}} \approx 1$  corresponding to the channel radius  $R_i^{\text{ch}} \approx 5$  fm. As is seen from Fig. 3c, the contribution of the peripheral partial waves to the reaction amplitude is suppressed strongly, whereas the main contribution to the amplitude comes to the low partial waves in the vicinity of  $l_i \sim 1$ . The analogous dependence occurs for other considered incident proton energies. This result is apparently not accidental and can be explained as: for rather low

sub-barrier energies ( $k_i \rightarrow 0$ ), the position of the nearest singularity  $\xi$  moves away from the right boundary ( $\cos \theta=1$ ) of the physical ( $-1 \leq \cos \theta \leq 1$ ) region ( $\xi \gg 1$  and  $\tau \gg 1$ ). Therefore, as is seen from the fourth column of Table 3, due to a presence of the factor  $\exp(-l_i \ln \tau) / \sqrt{\xi^2 - 1}$  in Eqs. (A2) – (A4), the calculated values of the peripheral partial amplitudes for  $l_i \gg 1$  become extremely smaller at sub-barrier energies than those at above-barrier energies for which the position of the singularity  $\xi$  is located rather close to the aforementioned boundary (see the fourth line of Table 3 and Fig. 3c).

It follows from here that the influence of the three-body Coulomb effects in the initial, intermediate and final states of the considered above-barrier reactions on the peripheral partial amplitudes of the reaction amplitude can not be ignored even for the “non-dramatic” case. One notes that this influence is ignored in the calculations of the “post”-approximation and the “post” form of the DWBA performed in [7] and [8], respectively. In this connection, it should be noted that this assertion is related also to the calculations of the dispersion peripheral model for the peripheral proton transfer reactions performed in [35] with taking into account only the mechanism described by the pole diagram in Fig. 1a.

The results of the analysis of the experimental differential cross sections [8, 31, 33, 34] performed using Eq. (51) and of the ANC values derived for  ${}^9\text{Be} + p \rightarrow {}^{10}\text{B}_i$  ( $i=0-3$ ),  ${}^{16}\text{O} + p \rightarrow {}^{17}\text{F}_i$  ( $i=0$  and  $1$ ) and  ${}^{16}\text{O} + t \rightarrow {}^{19}\text{F}(\text{g.s.})$  and their comparison with those of the conventional DWBA obtained by other authors in Refs. [8, 31, 33] will be reported in the next paper. Besides, there, the results of application of the ANC values above for the nuclear-astrophysical  ${}^9\text{Be}(p, \gamma){}^{10}\text{B}$ ,  ${}^{16}\text{O}(p, \gamma){}^{17}\text{F}$  and  ${}^{19}\text{F}(p, \alpha){}^{16}\text{O}$  reactions will also be presented.

## VII. CONCLUSION

Within the three-body Schrödinger formalism combined with the dispersion theory, a new asymptotic theory is proposed for the peripheral sub- and above-barrier charged-particle transfer  $A(x, y)B$  reaction, which is related to the “non-dramatic” case, where  $x=(y+a)$ ,  $B=(A+a)$  and  $a$  is the transferred particle. There, the contribution of the three-body ( $A$ ,  $a$  and  $y$ ) Coulomb dynamics of the transfer mechanism to the main reaction amplitude is taken into account in the correct manner within the framework of the dispersion theory. While, an influence of the Coulomb-nuclear distortion effects in the entrance and exit channels are kept in mind as it is done in the conventional DWBA. In the asymptotic theory proposed, the contribution of the three-body Coulomb effects in the initial, intermediate and final states to the amplitude for the main pole mechanism is taken correctly into account in all orders over the Coulomb polarization potential  $V_{i,f}^C$  of the perturbation theory. Therefore, it can be considered as a generalization of the “post”-approximation and the post form of the conventional DWBA.

The explicit forms of the generalized DWBA amplitude, the peripheral partial amplitudes at  $l_i \gg 1$  and  $l_f \gg 1$  and respective the differential cross section have been obtained. They are directly expressed in the terms of the product of the ANC’s (or respective the NVC’s) for  $y+a \rightarrow x$  and  $A+a \rightarrow B$  being adequate to the physics of the charge particle surface reaction. In the amplitude derived, the contributions both of the rather low partial waves and of the peripheral partial ones are taken into account in the pole approximation valid for the channel radius  $R_i^{\text{ch}} \gtrsim R_N$ . It makes it possible to consider simultaneously both the sub-barrier transfer reaction and the above-barrier one. The calculations of the partial amplitudes has been

perform for the specific above- and sub-barrier peripheral reactions corresponding to the proton and triton transfer mechanisms, respectively. It is shown quantitatively that it is necessary to take into account the three-body Coulomb dynamics in the main pole transfer mechanism for calculation of the amplitude and the differential cross section where the partial amplitudes with  $l_i \gg 1$  and  $l_f \gg 1$  provide essential contribution at least in the angular range of the main peak of the angular distribution of the differential cross section.

## ACKNOWLEDGEMENT

The authors are deeply grateful to L. D. Blokhintsev for discussions and constructive suggestions. This work has been supported in part by the Academy of Sciences of the Republic of Uzbekistan.

## APPENDIX A: Behavior of the pole-approximation and the "post" form of the DWBA amplitudes near $\cos \theta \rightarrow \xi$ and their the peripheral partial amplitudes at $l_i \gg 1$ . The approximate forms of the CRFs and the "dramatic" case

Here, the explicit approximate forms for the behavior of the pole-approximation and the post form of the DWBA amplitudes near  $\cos \theta \rightarrow \xi$  and the corresponding peripheral partial amplitudes at  $l_i \gg 1$  are presented. Besides, below, we will find out the main reason of a provenance of the "dramatic" case for the CRF values calculated at the values of the Coulomb parameters  $\eta_x$ ,  $\eta_B$  or  $\eta_x + \eta_B$  near to a natural number.

According to Refs. [12, 13] and [14], the explicit expressions of the  $\tilde{M}_{\text{pole}}^{(s)}(E_i, \cos \theta)$ , which determine the behaviors of the pole  $M_{\text{pole}}^{\text{DW}}(E_i, \cos \theta)$  amplitude near the singularity at  $\cos \theta = \xi$ , and the corresponding peripheral partial amplitudes for  $l_i \gg 1$  have the forms as

$$\tilde{M}_{\text{pole}}^{(s)}(E_i, \cos \theta) = \frac{m_a}{k_i k_f} \frac{G_{Aa} G_{ay}}{(\xi - \cos \theta)^{1 - \eta_{xB} + i\eta_{if}}}. \quad (\text{A1})$$

and

$$\begin{aligned} \tilde{M}_{l_i; \text{pole}}^{(s)}(E_i) &\approx \sqrt{\pi} \frac{m_a}{k_i k_f} G_{Aa} G_{ay} \frac{(\xi^2 - 1)^{(\eta_{xB} - i\eta_{if})/2}}{\Gamma(1 - \eta_{xB} + i\eta_{if}) \sqrt{\tau^2 - 1}} \\ &\times \frac{e^{-l_i \ln \tau}}{l_i^{1/2 + \eta_{xB} - i\eta_{if}}} \end{aligned} \quad (\text{A2})$$

for  $l_i \gg 1$ , respectively, where  $\tau = \xi + \sqrt{\xi^2 - 1}$ ,  $\eta_{xB} = \eta_x + \eta_B$  and  $\eta_{if} = \eta_i + \eta_f$ , and  $\eta_i$  ( $\eta_f$ ) is the Coulomb parameter in the entrance (exit) channel. From Eqs. (13) - (15), (A1) and (A2) we can obtain the explicit forms of the peripheral partial amplitudes for the  $M_{\text{pole}}^{(s) \text{DW}}(E_i, \cos \theta)$  and  $M_{\text{post}}^{(s) \text{DW}}(E_i, \cos \theta)$  amplitudes. They have the forms as

$$M_{l_i; \text{pole}}^{\text{DW}} \approx \tilde{N}_{\text{pole}}^{\text{DW}} \tilde{M}_{l_i; \text{pole}}^{(s)}(E_i) \quad (\text{A3})$$

and

$$M_{l_i; \text{post}}^{\text{DW}} \approx \tilde{N}_{\text{post}}^{\text{DW}} \tilde{M}_{l_i; \text{pole}}^{(s)}(E_i), \quad (\text{A4})$$

where  $\tilde{N}_{\text{pole}}^{\text{DW}} = N_{\text{pole}}^{\text{DW}}/\Gamma(1 - \eta_{xB} + i\eta_{if})$  and  $\tilde{N}_{\text{post}}^{\text{DW}} = N_{\text{post}}^{\text{DW}}/\Gamma(1 - \eta_{xB} + i\eta_{if})$ .

The explicit forms of the  $N_{\text{pole}}^{\text{DW}}$  and  $N_{\text{post}}^{\text{DW}}$  CRF's contain the integrals over the variable  $t$  ( $0 \leq t \leq 1$ ) with the cumbersome integrand functions. As seen from Ref. [13], the dependence of the integrand functions on the vertex Coulomb parameters ( $\eta_x$  and  $\eta_B$ ) and the Coulomb parameters in the entrance and exit channels ( $\eta_i$  and  $\eta_f$ ) are presented in the factorized forms as  $F_{\eta_x \eta_B}^{(j)}(t) \tilde{F}_{\eta_i \eta_f}^{(j)}(t)$  for the integral corresponding to the  $N_{\text{pole}}^{\text{DW}}$  ( $j=1$ ) and that corresponding to  $N_{\text{post}}^{\text{DW}}$  ( $j=2$ ). One notes that the  $\tilde{F}_{\eta_i \eta_f}^{(j)}(t)$  functions are regular at the points  $t=0$  and 1, whereas the  $F_{\eta_x \eta_B}^{(j)}(t)$  functions have the integrable singularities at these points. In this case, the approximated explicit forms for the  $N_{\text{pole}}^{\text{DW}}$  and  $N_{\text{post}}^{\text{DW}}$  CRFs can be obtained from the expressions (14) and (26) of Ref. [13], since the modulus of the  $\tilde{F}_{\eta_i \eta_f}^{(j)}(t)$  functions change slower than the  $F_{\eta_x \eta_B}^{(j)}(t)$  functions within the integration interval. Therefore, the regular  $\tilde{F}_{\eta_i \eta_f}^{(j)}(t)$  functions can be taken out from under the integrations in Eqs. (14) and (26) of [13] at the point  $t=0$  being a singular point (a branch one) for the other  $\tilde{F}_{\eta_x \eta_B}^{(j)}(t)$  functions ( $j=1$  and 2). As a result, the expressions for the CRF's above can be reduced to the forms

$$N_{\text{pole}}^{\text{DW}} \approx N_{\text{pole}}^{(ap); \text{DW}} = \Gamma(1 - \eta_{xB} + i\eta_{if})(\xi^2 - 1)^{i\eta_{if}/2} \left( \frac{\lambda_B}{\lambda_x} \right)^{\eta_x} \mathcal{D}_{\eta_x \eta_B \eta_i \eta_f}(k_i, k_f) I_{\text{pole}}(\eta_x, \eta_B) \quad (\text{A5})$$

and

$$N_{\text{post}}^{\text{DW}} \approx N_{\text{post}}^{(ap); \text{DW}} = N_{\text{pole}}^{(ap); \text{DW}} + N_{\Delta}^{(ap); \text{DW}} - N_f^{(ap); \text{DW}}, \quad (\text{A6})$$

$$N_{\Delta}^{\text{DW}} \approx N_{\Delta}^{(ap); \text{DW}} = \mu_{ay} \eta_{yA} (2E_{yA}/\mu_{yA})^{1/2} \Gamma(1 - \eta_{xB} + i\eta_{if})(\xi^2 - 1)^{i\eta_{if}/2} \left( \frac{\lambda_B}{\lambda_x} \right)^{\eta_x} \times \mathcal{D}_{\eta_x \eta_B \eta_i \eta_f}(k_i, k_f) I_1(\eta_x, \eta_B), \quad (\text{A7})$$

$$N_f^{\text{DW}} \approx N_f^{(ap); \text{DW}} = \mu_{ay} (\eta_f k_f / \mu_f) \Gamma(1 - \eta_{xB} + i\eta_{if})(\xi^2 - 1)^{i\eta_{if}/2} \left( \frac{\lambda_B}{\lambda_x} \right)^{\eta_x} \times \mathcal{D}_{\eta_x \eta_B \eta_i \eta_f}(k_i, k_f) I_2(\eta_x, \eta_B). \quad (\text{A8})$$

Herein:  $E_{yA} = (m_{Ax} E_i + m_B \varepsilon_{Aa} + m_x \varepsilon_{ay})/m_{yA}$  is the relative kinetic energy of the  $A$  and  $y$  cores in the intermediate state,

$$\mathcal{D}_{\eta_x \eta_B \eta_i \eta_f}(k_i, k_f) = C(\eta_i, \eta_f) \left( \frac{k_{i1} k_f}{2i\kappa_{ay}^2} \right)^{\eta_x} \left( \frac{k_i k_{f1}}{2i\kappa_{Aa}^2} \right)^{\eta_B} \quad (\text{A9})$$

$$I_{\text{pole}}(\eta_x, \eta_B) = \eta_x \int_0^1 dt \frac{(1 - \tilde{c}t)^{\eta_{xB}-1}}{t^{1+\eta_x} (1-t)^{\eta_B}}, \quad (\text{A10})$$

$$I_j(\eta_x, \eta_B) = \int_0^1 dt \frac{(1 - \tilde{c}t)^{\eta_{xB}-1}}{t^{\eta_x} (1-t)^{\eta_B} \sqrt{\chi_j(t)}}. \quad (\text{A11})$$

Herein:  $\tilde{c} = 1 - \lambda_x/\lambda_B < 1$  ( $\lambda_x = m_y/m_x$  and  $\lambda_B = m_A/m_B$ ) and

$$\chi_j(t) = a_j t^2 + b_j t + c_j \quad (\text{A12a})$$

in which

$$\begin{aligned}
a_1 &= m_a(\kappa_{ay}^2 - \kappa_{Aa}^2)/m_B - m_a^2\kappa_{Aa}^2/m_A m_B - (m_a m_{By} k_i / m_x \sqrt{m_A m_B})^2, \\
a_2 &= m_a m_{AB}(\kappa_{ay}^2 - \kappa_{Aa}^2)/m_B^2 - (m_a m_{By} k_i / m_x m_B)^2, \\
b_1 &= m_A(\kappa_{ay}^2 - \kappa_{Aa}^2)/m_B + m_a^2\kappa_{Aa}^2/m_A m_B + (m_a m_{By} k_i / m_x \sqrt{m_A m_B})^2, \\
b_2 &= m_A^2(\kappa_{ay}^2 - \kappa_{Aa}^2)/m_B^2 + m_a m_{AB} \kappa_{Aa}^2 / m_B^2 + (m_a m_{By} k_i / m_x m_B)^2, \\
c_1 &= \kappa_{Aa}^2, \quad c_2 = m_A^2 \kappa_{Aa}^2 / m_B^2
\end{aligned} \tag{A13}$$

and

$$C(\eta_i, \eta_f) = \exp[-(\eta_f - \eta_i)\tilde{\varphi} - (\eta_i + \eta_f)\tilde{\psi}], \tag{A14}$$

where

$$\tilde{\varphi} = \tan^{-1} \left( \frac{k_i - k_{f1}}{\kappa_{Aa}} \right), \quad \tilde{\psi} = \tan^{-1} \left( \frac{\kappa_{Aa}}{k_i + k_{f1}} \right). \tag{A15}$$

By using this case, we note that there are misprints in expression (14) of [13]. There, in the right-hand side of the equation for  $\tilde{N}(\eta_\alpha, \eta_\beta, \eta_i, \eta_f)$ , the factor  $(\lambda_\beta/\lambda_\alpha)^{\eta_\alpha}$  ( $\equiv (\lambda_B/\lambda_x)^{\eta_x}$  in Eq.(A11)) is omitted and factor  $e^{-\pi\eta}$  should be substituted by that of  $e^{-\pi\eta/2}$  ( $\eta \equiv \eta_{if}$ ).

In Eq. (A9), the Coulomb  $C(\eta_i, \eta_f)$  factor arises because of the aforesaid approximate taking into account of the Coulomb distorted effects in the entrance and exit channels. One notes that this factor coincides with that obtained in [40] from the approximate amplitude of the sub-barrier neutron transfer reaction derived within the diffraction model. Besides, as is seen from Eqs. (A12a) and (A13),  $\chi_j(t) > 0$  for  $0 \leq t \leq 1$  ( $j=1$  and  $2$ ) and  $\chi_1(0) = \kappa_{Aa}^2$ ,  $\chi_2(0) = m_A^2 \kappa_{Aa}^2 / m_B^2$  and  $\chi_j(1) = a_j + b_j + c_j = \kappa_{ay}^2$  as well as  $a_j < 0$  and  $b_j > 0$ , since  $k_i > \kappa_{ay}$  and  $k_i > \kappa_{Aa}$ .

We now consider the integrals (A10) and (A11). Integration in Eq. (A10) can be easily done by using formula 3.197(4) of [38]. It results in the expression

$$I_{\text{pole}}(\eta_x, \eta_B) = - \left( \frac{\lambda_x}{\lambda_B} \right)^{\eta_x} F_C(\eta_x, \eta_B), \tag{A16}$$

where

$$F_C(\eta_x, \eta_B) = \frac{\Gamma(1 - \eta_x)\Gamma(1 - \eta_B)}{\Gamma(1 - \eta_x - \eta_B)}. \tag{A17}$$

To take the integral (A11), firstly, the  $\chi_j(t)$  function should be presented to the form

$$\chi_j(t) = a_j(t - t_j^{(1)})(t - t_j^{(2)}), \tag{A12b}$$

where  $t_j^{(k)}$  ( $k=1$  and  $2$ ) are the solutions of the equations  $\chi_j(t)=0$  for which  $t_j^{(1)} > 1$  and  $t_j^{(2)} < 0$  ( $j=1$  and  $2$ ). Then, using Eq. (A12b), the  $[\chi_j(t)]^{-1/2}$  functions can be expanded in the binomial series at the points  $t = t_{j;0} = b_j/2|a_j| < 1$ , which are the extremum (minimum) points of the functions above. The power expansion for the  $[\chi_j(t)]^{-1/2}$  functions is reduced to the form as

$$[\chi_j(t)]^{-1/2} = f_0^{(j)} + \sum_{n=2}^{\infty} f_n^{(j)}(t - t_{j;0})^n. \tag{A18}$$

Herein

$$f_n^{(j)} = (-1)^n \frac{2|a_j|^{n+1/2}}{D_j^{(n+1)/2}} \sum_{k=0}^n (-1)^k \frac{(2k-1)!![2(n-k)-1]!!}{k!(n-k)!}, \quad (\text{A19})$$

$f_0^{(j)} = [\chi_j(t_{j;0})]^{-1/2} = (|a_j|/D_j)^{1/2}$  and  $[\chi_j'(t_{j;0})]^{-1/2} = 0$  in which the prime is marked a derivation from the  $[\chi_j(t)]^{-1/2}$  function, and  $(-1)!! = 1$ .

Inserting Eq. (A18) in Eq. (A11) and using formulae 3.197(3) and 3.211 from [38] in the obtained expression, for  $I_j(\eta_x, \eta_B)$  we derive the following form

$$I_j(\eta_x, \eta_B) = \frac{F_C(\eta_x, \eta_B)}{(1 - \eta_{xB})} \tilde{I}_j(\eta_x, \eta_B) \quad (\text{A20})$$

where

$$\tilde{I}_j(\eta_x, \eta_B) = 2 \left( \frac{|a_j|}{D_j} \right)^{1/2} + \sum_{n=2}^{\infty} \frac{f_n^{(j)}}{n!} F_1(1 - \eta_x, -n, 1 - \eta_{xB}; 2 - \eta_{xB}; t_{j;0}^{-1}, \tilde{c}). \quad (\text{A21})$$

Herein:

$$F_1(1 - \eta_x, -n, 1 - \eta_{xB}; 2 - \eta_{xB}; t_{j;0}^{-1}, \tilde{c}) = \sum_{q=0}^n \frac{n!}{q!(n-q)!} (-t_{j;0})^{-q} \\ \times \frac{\Gamma(1+q-\eta_x)}{\Gamma(1-\eta_x)} \frac{\Gamma(2-\eta_{xB})}{\Gamma(2+q-\eta_{xB})} F(1-\eta_{xB}, 1+q-\eta_x; 2+q-\eta_{xB}; \tilde{c}) \quad (\text{A22})$$

is the hypergeometric function of two variables [38], and  $F(a, b; c; \tilde{x})$  is the known hypergeometric function.

Inserting Eqs. (A16) and (A17) in Eq. (A5), and Eqs. (A7), (A8) and (A20) in Eq. (A6) the  $N_{\text{pole}}^{\text{DW}}$  and  $N_{\text{post}}^{\text{DW}}$  CRF's can be reduced to the forms as

$$N_{\text{pole}}^{\text{DW}} \approx N_{\text{pole}}^{(ap); \text{DW}} = -\Gamma(1 - \eta_{xB} + i\eta_{if})(\xi^2 - 1)^{i\eta_{if}/2} F_C(\eta_x, \eta_B) \mathcal{D}_{\eta_x \eta_B \eta_i \eta_f}(k_i, k_f) \quad (\text{A23})$$

and

$$N_{\text{post}}^{\text{DW}} \approx N_{\text{post}}^{(ap); \text{DW}} = N_{\text{pole}}^{(ap); \text{DW}} \left\{ 1 - \frac{\mu_{ay}(\lambda_B/\lambda_x)^{\eta_x}}{(1 - \eta_{xB})} \right. \\ \left. \times [\eta_{yA}(2E_{yA}/\mu_{yA})^{1/2} \tilde{I}_1(\eta_x, \eta_B) - (\eta_f k_f/\mu_f) \tilde{I}_2(\eta_x, \eta_B)] \right\}. \quad (\text{A24}).$$

As is seen from Eqs. (A23) and (A24), the approximate allowance of the Coulomb distortions in the entrance and exit channels in the expressions for the  $N_{\text{pole}}^{\text{DW}}$  and  $N_{\text{post}}^{\text{DW}}$  CRF's makes us it possible to derive their explicit forms in which the factors, depending both on the Coulomb  $\eta_x$  and  $\eta_B$  parameters and on the Coulomb  $\eta_i$  and  $\eta_f$  ones, are separated. The explicit approximate forms for the  $M_{\text{pole}}^{(s)\text{DW}}(E_i, \cos\theta)$  and  $M_{\text{post}}^{(s)\text{DW}}(E_i, \cos\theta)$  amplitudes can be obtained from Eqs. (13), (14) and (15) by mean of replacement of the  $N_{\text{pole}}^{\text{DW}}$  and  $N_{\text{post}}^{\text{DW}}$  CRF's by those given in Eqs. (A23) and (A24), respectively. Similar to Eqs. (A1) and (A2), the amplitudes above determine the behavior of peripheral partial amplitudes for  $l_i \gg 1$ , which have the forms as

$$M_{\text{pole}; l_i}^{\text{DW}}(E_i) \approx M_{\text{pole}; l_i}^{(ap); \text{DW}}(E_i) = \sqrt{\pi} \frac{m_a}{k_i k_f} G_{Aa} G_{ay} \frac{(\xi^2 - 1)^{\eta_{xB}/2}}{\sqrt{\tau^2 - 1}}$$

$$\times F_C(\eta_x, \eta_B) \mathcal{D}_{\eta_x \eta_B \eta_i \eta_f}(k_i, k_f) \frac{e^{-l_i \ln \tau}}{l_i^{1/2 + \eta_{xB} - i\eta_{if}}} \quad (\text{A25})$$

and

$$M_{\text{post}; l_i}^{\text{DW}}(E_i) \approx M_{\text{post}; l_i}^{(\text{ap}); \text{DW}}(E_i) = \mathcal{R}_{\text{post}}^{(\text{ap}); \text{DW}} M_{\text{pole}; l_i}^{(\text{ap}); \text{DW}}(E_i) \quad (\text{A26})$$

for  $l_i \gg 1$ , where  $G_{Aa} \equiv G_{Aa; l_B j_B}$  and  $G_{ay} \equiv G_{ay; l_x j_x}$ , and  $N_{\text{post}}^{(\text{ap}); \text{DW}}$  is determined by Eq. (A24), and  $\mathcal{R}_{\text{post}}^{(\text{ap}); \text{DW}} = N_{\text{post}}^{(\text{ap}); \text{DW}} / N_{\text{pole}}^{(\text{ap}); \text{DW}}$ .

According to [12, 13], the CRF  $N^{\text{TBDM}}$  for the  $M^{(s)\text{TBDM}}(E_i, \cos\theta)$  amplitude, given by Eq. (16), can be presented in the form

$$N^{\text{TBDM}} = -(k_{i1} k_f / 2i\kappa_{ay}^2)^{\eta_x} (k_i k_{f1} / 2i\kappa_{Aa}^2)^{\eta_B} (\xi^2 - 1)^{i\eta_{if}/2} \\ \times \Gamma(1 - \eta_{xB} + i\eta_{if}) F_C(\eta_x, \eta_B) N(\eta_x, \eta_B, \eta_i, \eta_f), \quad (\text{A27})$$

$$N(\eta_x, \eta_B, \eta_i, \eta_f) = F_C^{-1}(\eta_x, \eta_B) \Delta_{\eta_{yA}}(k_i, k_f) \tilde{\Delta}_{\eta_i \eta_f}(k_i, k_f), \quad (\text{A28})$$

$$\Delta_{\eta_{yA}}(k_i, k_f) = e^{-2\eta_{yA}\varphi_{yA}}, \quad \tilde{\Delta}_{\eta_i \eta_f}(k_i, k_f) = \exp(-\eta_i\varphi_i - \eta_f\varphi_f), \quad (\text{A29})$$

$$\varphi_{yA} = \tan^{-1} \frac{(m_a m_{yA} E_{yA})^{1/2}}{(m_x m_A \varepsilon_{ay})^{1/2} + (m_B m_y \varepsilon_{Aa})^{1/2}}, \quad (\text{A30})$$

$$\varphi_i = \tan^{-1} \left( \frac{k_{f1}^2 - k_i^2}{2k_i \kappa_{Aa}} \right), \quad \varphi_f = \tan^{-1} \left( \frac{k_{i1}^2 - k_f^2}{2k_{i1} \kappa_{ay}} \right). \quad (\text{A31})$$

The behavior of the peripheral partial amplitudes of the  $M^{(s)\text{TBDM}}(E_i, \cos\theta)$  amplitude for  $l_i \gg 1$  has the form as [12, 13]

$$M_{l_i}^{\text{TBDM}}(E_i) \approx \sqrt{\pi} \frac{m_a}{k_i k_f} G_{Aa} G_{ay} \frac{(\xi^2 - 1)^{(\eta_{xB} - i\eta_{if})/2}}{\sqrt{\tau^2 - 1}} \tilde{N}^{\text{TBDM}} \frac{e^{-l_i \ln \tau}}{l_i^{1/2 + \eta_{xB} - i\eta_{if}}}. \quad (\text{A32})$$

One notes that, the three-body CRF  $N(\eta_x, \eta_B, \eta_i, \eta_f) (\equiv N)$  (A28) arises due to correct taking into account both of the three-body Coulomb dynamics in the main transfer mechanism and of the Coulomb interactions in the entrance and exit states. As shown in Refs. [12] and [41], the factors  $F_C^{-1}(\eta_x, \eta_B)$  and  $\Delta_{\eta_{yA}}(k_i, k_f)$  in Eq. (A28) by-turn arise as a result of taking into account all possible subsequent mutual Coulomb interactions of the transferred particle  $a$  with the cores  $A$  and  $y$  and of the cores  $A$  and  $y$ , respectively, in the main transfer mechanism. Whereas the factor  $\tilde{\Delta}_{\eta_i \eta_f}(k_i, k_f)$  arises due to Coulomb interaction in the initial and final states. As is seen from the expressions (A27) and (A28), in Eq. (A27), the contribution of the  $F_C(\eta_x, \eta_B)$  factor to the  $N^{\text{TBDM}}$  CRF is compensated by an appearance of the factor  $F_C^{-1}(\eta_x, \eta_B)$  in the three-body Coulomb factor  $N$ . The  $F_C(\eta_x, \eta_B)$  factor arises because of the vertex Coulomb effects in the three-ray vertexes of the pole diagram of Fig. 1a, which corresponds to the pure pole amplitude [12, 35]. Besides, the expression (16) coincides with the behavior of the pure pole amplitude (Fig. 1a) near a vicinity of the singularity at  $\cos\theta = \xi$  when a contribution of the three-body Coulomb effects in the three-body DWBA amplitude is ignored, i.e., the three-body Coulomb factor  $N$  should set equal to unity in Eq. (A27).

We now discuss the main reason of a provenance of the ‘‘dramatic’’ case mentioned above. It arises because of taking into account only the single-Coulomb rescattering of the transferred particle  $a$  with the cores  $A$  and  $y$  in the pole-approximation and the ‘‘post’’ form of the DWBA at values of either  $\eta_x$  or  $\eta_B$  or  $\eta_{xB}$  are in the vicinity of a natural number. In this case, as it is seen from Eqs. (A23) and (A24) as well as Eqs. (A27) and (A28), the difference between the CRF’s  $N_{\text{pole}}^{\text{DW}}$ ,  $N_{\text{post}}^{\text{DW}}$  and  $N^{\text{TBDM}}$  (or  $\tilde{N}_{\text{pole}}^{\text{DW}}$ ,  $\tilde{N}_{\text{post}}^{\text{DW}}$  and  $\tilde{N}^{\text{TBDM}}$ ) becomes significant. It is due to a presence of the vertex Coulomb  $F_C(\eta_x, \eta_B)$  and  $F_C(\eta_x, \eta_B)/(1 - \eta_{xB})$  factors in Eqs. (A23) and (A24), respectively, whereas they are absent in the  $N^{\text{TBDM}}$  (or  $\tilde{N}^{\text{TBDM}}$ ) CRF in Eqs. (A27) and (A28). This means that the power expansion over the Coulomb polarization potential  $\Delta V_{i,f}^C$  in the transition operator of Eqs. (10) and (11), which correspond to the zero- and first orders of the perturbation theory over  $\Delta V_{i,f}^C$ , has a poor convergence in the ‘‘dramatic’’ case.

Therefore, in the ‘‘dramatic’’ case, the next terms ( $\Delta V_f^C G_C \Delta V_i^C$ ) of the transition operator in the series in  $\Delta V_{f,i}^C$  should directly be taken into account in the  $M^{\text{TBBDW}}(E_i, \cos\theta)$  amplitude. Since each of the terms of them has the identical behaviour as that for the  $M_{\text{post}}^{(s)\text{DW}}(E_i, \cos\theta)$  amplitude [13], one obtains the expression

$$\Delta M^{\text{TBBDW}}(E_i, \cos\theta) \approx \Delta M^{(s)\text{TBBDW}}(E_i, \cos\theta) = \Delta N^{\text{TBBDW}} \tilde{M}_{\text{pole}}^{(s)}(E_i, \cos\theta), \quad (\text{A33})$$

where  $\Delta N^{\text{TBBDW}}$  is the CRF corresponding to the  $\Delta M^{\text{TBBDW}}(E_i, \cos\theta)$  amplitude. Then, the expression for the main singular term of the  $M^{\text{TB}}(E_i, \cos\theta)$  amplitude near  $\cos\theta = \xi$  can be presented in the form

$$M^{\text{TB}}(E_i, \cos\theta) \approx M^{(s)\text{TB}}(E_i, \cos\theta) = \mathcal{R}^{\text{TB}}(E_i) M_{\text{pole}}^{(s)}(E_i, \cos\theta), \quad (\text{A34})$$

where

$$\mathcal{R}^{\text{TB}}(E_i) = N^{\text{TB}}(E_i)/N_{\text{pole}}^{\text{DW}}(E_i) \quad (\text{A35})$$

and

$$N^{\text{TB}} = N_{\text{post}}^{\text{DW}} + \Delta N^{\text{TBBDW}}. \quad (\text{A36})$$

As a result, from Eqs. (16) and (A34), the behavior of the exact three-body  $M^{\text{TB}}(E_i, \cos\theta)$  DWBA amplitude near the singularity at  $\cos\theta = \xi$  is presented in the form

$$M^{\text{TB}}(E_i, \cos\theta) \approx M^{(s)\text{TB}}(E_i, \cos\theta) = \tilde{\mathcal{R}}^{\text{TB}}(E_i) M_{\text{pole}}^{(s)}(E_i, \cos\theta). \quad (\text{A37})$$

Herein:

$$\tilde{\mathcal{R}}^{\text{TB}}(E_i) = N^{\text{TBDM}}(E_i)/N^{\text{TB}}(E_i) = \tilde{N}^{\text{TBDM}}(E_i)/\tilde{N}^{\text{TB}}(E_i), \quad (\text{A38})$$

which is valid for the ‘‘dramatic’’ case, where  $\tilde{N}^{\text{TB}}(E_i) = N^{\text{TB}}(E_i)/\Gamma(1 - \eta_{xB} + i\eta_{if})$ .

One notes that, in reality, the expressions (A34)–(A38) are valid simultaneously both for the ‘‘dramatic’’ case and for the ‘‘non-dramatic’’ one. Therefore, Eqs. (A34)–(A36) are more accurate than the expression (17). Consequently, they may also be used for testing the accuracy of Eq. (17). Hence, a knowledge of the explicit form of the  $\Delta N^{\text{TBBDW}}$  CRF is required. But, the task of direct finding the explicit form of the  $\Delta N^{\text{TBBDW}}$  CRF is fairly difficult because of the presence of the three-body Coulomb operator  $G_C$  in the transition operator of Eq. (12) and, so, it requires a special consideration. At present such work is in progress within the cycle of

works, which are carried by us, on a development of the asymptotic theory for the peripheral reaction (1), which must really involve both the “dramatic” case and the “non-dramatic” one.

## APPENDIX B: Formulae and expressions

Here we present the necessary formulae and expressions.

The matrix element  $M_{Aa}(\mathbf{q}_{Aa})$  of the virtual decay  $B \rightarrow A + a$  is related to the overlap function  $I_{Aa}(\mathbf{r}_{Aa})$  as [9]

$$\begin{aligned} M_{Aa}(\mathbf{q}_{Aa}) &= N_{Aa}^{1/2} \int e^{-i\mathbf{q}_{Aa}\mathbf{r}_{Aa}} V_{Aa}(\mathbf{r}_{Aa}) I_{Aa}(\mathbf{r}_{Aa}) d\mathbf{r}_{Aa} \\ &= -N_{Aa}^{1/2} \left( \frac{q_{Aa}^2}{2\mu_{Aa}} + \varepsilon_{Aa} \right) \int e^{-i\mathbf{q}_{Aa}\mathbf{r}_{Aa}} I_{Aa}(\mathbf{r}_{Aa}) d\mathbf{r}_{Aa} \\ &= \sqrt{4\pi} \sum_{l_B \mu_B j_B \nu_B} C_{j_B \nu_B J_A M_A}^{J_B M_B} C_{l_B \mu_B J_a M_a}^{j_B \nu_B} G_{Aa; l_B j_B}(q_{Aa}) Y_{l_B \mu_B}(\hat{\mathbf{q}}_{Aa}), \end{aligned} \quad (B1)$$

where  $G_{Aa; l_B j_B}(q_{Aa})$  is the vertex formfactor for the virtual decay  $B \rightarrow A + a$ ,  $\mathbf{q}_{Aa}$  is the relative momentum of the  $A$  and  $a$  particles and  $G_{Aa; l_B j_B} \equiv G_{Aa; l_B j_B}(i\kappa_{Aa})$ , i.e., the NVC coincides with the vertex formfactor  $G_{Aa; l_B j_B}(q_{Aa})$  when all the  $B$ ,  $a$  and  $A$  particles are on-shell ( $q_{Aa} = i\kappa_{Aa}$ ). The same relations similar to Eq. (B1) hold for the matrix element  $M_{ay}(\mathbf{q}_{ay})$  of the virtual decay  $x \rightarrow y + a$  and the overlap function  $I_{ay}(\mathbf{r}_{ay})$ .

The partial-waves expansions for the distorted wave functions of relative motion of the nuclei in the initial and exit states of the reaction under consideration have the form as [20]

$$\begin{aligned} \Psi_{\mathbf{k}_i}^{(+)}(\mathbf{r}_i) &= \frac{4\pi}{k_i r_i} \sum_{l_i \mu_i} i^{l_i} e^{i\sigma_{l_i}} \Psi_{l_i}(k_i; r_i) Y_{l_i \mu_i}(\hat{\mathbf{r}}_i) Y_{l_i \mu_i}^*(\hat{\mathbf{k}}_i), \\ \Psi_{\mathbf{k}_i}^{*(-)}(\mathbf{r}_i) &= \frac{4\pi}{k_f r_f} \sum_{l_f \mu_f} i^{-l_f} e^{i\sigma_{l_f}} \Psi_{l_f}(k_f; r_f) Y_{l_f \mu_f}(\hat{\mathbf{r}}_f) Y_{l_f \mu_f}^*(\hat{\mathbf{r}}_f), \end{aligned} \quad (B2)$$

where  $\Psi_l(k; r)$  is the partial wave functions in the initial state or the final one.

The expansions of the  $r_{ay}^{l_x} Y_{l_x \sigma_x}(\hat{\mathbf{r}}_{ay})$  and  $r_{Aa}^{l_B} Y_{l_B \sigma_B}^*(\hat{\mathbf{r}}_{Aa})$  functions on the bipolar harmonics of the  $l_x$  rank and the  $l_B$  one have the forms as

$$\begin{aligned} r_{ay}^{l_x} Y_{l_x \sigma_x}(\hat{\mathbf{r}}_{ay}) &= \sqrt{4\pi} \sum_{\lambda_1 + \lambda_2 = l_x} \sum_{\tilde{\mu}_{\lambda_1} \tilde{\mu}_{\lambda_2}} \left( \frac{\hat{l}_x!}{\hat{\lambda}_1! \hat{\lambda}_2!} \right)^{1/2} \left( \frac{\mu_{Ax}}{m_a} r_i \right)^{\lambda_1} \left( -\frac{\mu_{Ax}}{\mu_{Aa}} r_f \right)^{\lambda_2} \\ &\quad \times C_{\lambda_1 \tilde{\mu}_{\lambda_1} \lambda_2 \tilde{\mu}_{\lambda_2}}^{l_x \mu_x} Y_{\lambda_1 \tilde{\mu}_{\lambda_1}}(\hat{\mathbf{r}}_i) Y_{\lambda_2 \tilde{\mu}_{\lambda_2}}(\hat{\mathbf{r}}_f) \end{aligned} \quad (B3)$$

and

$$\begin{aligned} r_{Aa}^{l_B} Y_{l_B \sigma_B}^*(\hat{\mathbf{r}}_{Aa}) &= \sqrt{4\pi} \sum_{\sigma_1 + \sigma_2 = l_B} \sum_{\tilde{\mu}_{\sigma_1} \tilde{\mu}_{\sigma_2}} \left( \frac{\hat{l}_B!}{\hat{\sigma}_1! \hat{\sigma}_2!} \right)^{1/2} \left( -\frac{\mu_{By}}{\mu_{ay}} r_i \right)^{\sigma_1} \left( \frac{\mu_{By}}{m_a} r_f \right)^{\sigma_2} \\ &\quad \times C_{\sigma_1 \tilde{\mu}_{\sigma_1} \sigma_2 \tilde{\mu}_{\sigma_2}}^{l_B \mu_B} Y_{\sigma_1 \tilde{\mu}_{\sigma_1}}^*(\hat{\mathbf{r}}_i) Y_{\sigma_2 \tilde{\mu}_{\sigma_2}}(\hat{\mathbf{r}}_f). \end{aligned} \quad (B4)$$

Eqs. (B3) and (B4) can be derived from (20) and

$$\int d\hat{\mathbf{r}}_i Y_{\sigma_1 \tilde{\mu}_{\sigma_1}}^*(\hat{\mathbf{r}}_i) Y_{l\mu_l}(\hat{\mathbf{r}}_i) Y_{l_i \mu_{l_i}}(\hat{\mathbf{r}}_i) Y_{\lambda_1 \tilde{\mu}_{\lambda_1}}(\hat{\mathbf{r}}_i) = (-1)^{\tilde{\mu}_l} \sum_{I \tilde{\mu}_I} \left( \frac{\hat{l}_i \hat{\lambda}_1 \hat{l} \hat{\sigma}_1}{(4\pi)^2 \hat{I} \hat{I}} \right)^{1/2} \\ \times C_{l_i 0 \lambda_1 0}^{I 0} C_{l 0 \sigma_1 0}^{I 0} C_{l_i \tilde{\mu}_{l_i} \lambda_1 \tilde{\mu}_{\lambda_1}}^{I \tilde{\mu}_I} C_{l - \tilde{\mu}_l \sigma_1 \tilde{\mu}_{\sigma_1}}^{I \tilde{\mu}_I}, \quad (B5)$$

$$\int d\hat{\mathbf{r}}_f Y_{l\mu_l}^*(\hat{\mathbf{r}}_f) Y_{\sigma_2 \tilde{\mu}_{\sigma_2}}^*(\hat{\mathbf{r}}_f) Y_{l_f \mu_{l_f}}(\hat{\mathbf{r}}_f) Y_{\lambda_2 \tilde{\mu}_{\lambda_2}}(\hat{\mathbf{r}}_f) = \sum_{L \tilde{\mu}_L} \left( \frac{\hat{l}_f \hat{\lambda}_2 \hat{l} \hat{\sigma}_2}{(4\pi)^2 \hat{L} \hat{L}} \right)^{1/2} \\ \times C_{l_f 0 \lambda_2 0}^{L 0} C_{l 0 \sigma_2 0}^{L 0} C_{l_f \tilde{\mu}_{l_f} \lambda_2 \tilde{\mu}_{\lambda_2}}^{L \tilde{\mu}_L} C_{l \tilde{\mu}_l \sigma_2 \tilde{\mu}_{\sigma_2}}^{L \tilde{\mu}_L}. \quad (B6)$$

The explicit form of  $M_{l_x l_B l_i l_f}^{\text{pole}}(E_i)$  entering Eq. (46) is given by

$$M_{l_x l_B l_i l_f}^{\text{pole}}(E_i) = e^{i(\sigma_i + \sigma_f)} (\hat{l}_i^2 \hat{l}_f)^{1/2} \\ \times \sum_{\sigma_1 + \sigma_2 = l_B} \sum_{\lambda_1 + \lambda_2 = l_x} \sum_{l l L} \hat{l} \begin{pmatrix} 2l_x \\ 2\lambda_1 \end{pmatrix}^{1/2} \begin{pmatrix} 2l_B \\ 2\sigma_1 \end{pmatrix}^{1/2} \bar{a}^{\lambda_1} \bar{b}^{\lambda_2} \bar{c}^{\sigma_1} \bar{d}^{\sigma_2} C_{l 0 \sigma_1 0}^{I 0} C_{l_i 0 \lambda_1 0}^{I 0} \quad (B7)$$

$$\times C_{l 0 \sigma_2 0}^{L 0} C_{l_f 0 \lambda_2 0}^{L 0} W(L \sigma_2 I \sigma_1; l l_B) X(\lambda_1 \lambda_2 l_x; l_i l_f J; l l l_B) \mathcal{B}_{l_x l_B l_i l_f \lambda_1 \sigma_1}^{\text{pole}}(k_i, k_f), \\ \mathcal{B}_{l_x l_B l_i l_f \lambda_1 \sigma_1}^{\text{pole}}(k_i, k_f) = (\eta_x / 4^{\eta_x + \eta_B}) (\kappa_{Aa} / 2)^{l_B} (\kappa_{ay} / 2)^{l_x} \kappa_{Aa} \kappa_{ay}^3 \\ \times \int_{R_i^{\text{ch}}}^{\infty} dr_i r_i^{\lambda_1 + \sigma_1 + 1} \Psi_{l_i}(r_i; k_i) \int_{R_f^{\text{ch}}}^{\infty} dr_f r_f^{\lambda_2 + \sigma_2 + 1} \Psi_{l_f}(r_f; k_f) \tilde{\mathcal{A}}_{l_B l_x l}(r_i, r_f), \quad (B8)$$

$$\tilde{\mathcal{A}}_{l_B l_x l}(r_i, r_f) = \frac{1}{2} \int_{-1}^1 dz P_l(z) F_{l_B}(r_{Aa}; \kappa_B, \eta_B - 1) F_{l_x}(r_{ay}; \kappa_{ay}, \eta_x), \quad (B9)$$

$$F_l(r; \kappa, \eta) = \frac{\pi^{1/2}}{\Gamma(l + \eta + 2)} \int_1^{\infty} dt e^{-\kappa r t} (t^2 - 1)^{l + \eta + 1}, \quad (B10)$$

where  $W(l_1 j_1 l_2 j_2; j_3 j_4)$  and  $X(\lambda_1 \lambda_2 l_x; l_i l_f J; l l l_B)$  are the standard Racah and Fano coefficients [39], respectively;  $R_i^{\text{ch}} = R_x + R_A$  and  $R_f^{\text{ch}} = R_y + R_B$  are the cutoff radii in the entrance and exit channels, respectively, which are determined only by the free parameter  $r_0$  since  $R_C = r_0 C^{1/3}$  in which  $C$  is a mass number of the nucleus  $C$ ;  $\binom{m}{n}$  is the binomial coefficient and  $\hat{j} = 2j + 1$ .

## References

- [1] L.D. Blokhintsev, R. Yarmukhamedov, S.V. Artemov, I. Boztosun, S.B. Igamov, Q.I. Tursunmakhtov, and M.K. Ubaydullaeva, *Uzb. J. Phys.* **12**, 217 (2010).
- [2] R. Yarmukhamedov, and Q.I. Tursunmahatov, *The Universe Evolution: Astrophysical and nuclear aspects. Edit. I. Strakovsky and L. D. Blokhintsev.* (New York, NOVA publishers, 2013), pp.219–270.
- [3] R.E. Tribble, C.A. Bertulani, M La Cognata, A.M. Mukhamedzhanov, and C. Spitaleri, *Rep. Prog. Phys.* **77**, 901 (2014).
- [4] L.D. Blokhintsev, V.I. Kukulin, A.A. Sakharuk, D.A. Savin, and E.V. Kuznetsova, *Phys. Rev. C* **48**, 2390 (1993).
- [5] S.B. Igamov, and R. Yarmukhamedov, *Nucl. Phys. A* **781**, 247 (2007).
- [6] R. Yarmukhamedov and D. Baye, *Phys. Rev. C* **84**, 024603 (2011).
- [7] S.V. Artemov, I.R. Gulamov, E.A. Zaparov, I.Yu. Zotov, and G. K. Nie, *Yad. Fiz.* **59**, 454 (1996)[*Phys. At. Nucl.* **59**, 428 (1996)].
- [8] A.M. Mukhamedzhanov, H.L. Clark, C.A. Gagliardi, Y.-W. Lui, L. Thache, R.E. Thibble, H.M. Xu, X.G. Zhou, V. Burjan, J. Cejpek, V. Kroha, and F. Carstoiu, *Phys. Rev. C* **56**, 1302 (1997).
- [9] L.D. Blokhintsev, I. Borbely, E.I. Dolinskii, *Phys. Part. Nucl.* **8**, 485 (1977).
- [10] I.S. Shapiro, *Theory of direct nuclear reactions* (Gosatomizdat, Moscow, 1963)(in Russian).
- [11] E.I. Dolinsky, P.G. Dzhamalov, A.M. Mukhamedzhanov, *Nucl.Phys.* **202**, 97 (1973).
- [12] G.V. Avakov, L.D. Blokhintsev, A.M. Mukhamedzhanov, and R. Yarmukhamedov, *Yad. Fiz.* **43**, 824 (1986)[*Sov. J. Nucl. Phys.* **43**, 524 (1986)].
- [13] Sh.S. Kajumov, A.M. Mukhamedzhanov, R. Yarmukhamedov, and I. Borbely, *Z. Phys. A* **336**, 297 (1990).
- [14] V.S. Popov, *Zh. Èksp. Teor. Fiz.* **47**, 2229 (1964)[*Sov. Phys. JETP* **20**, 1494 (1965)].
- [15] Sh.S. Kajumov, A.M. Mukhamedzhanov, and R. Yarmukhamedov, *Z. Phys. A* **331**, (1988) 315.
- [16] R. Yarmukhamedov, *Yad. Fiz.* **60**, 1017 (1997)[*Phys. At. Nucl.* **60**, 910 (1997)].
- [17] S.B. Igamov, M.C. Nadyrbekov and R. Yarmukhamedov, *Phys. At. Nucl.* **70**, 1694 (2007).
- [18] E.I. Dolinskii, A.M. Mukhamedzhanov, R. Yarmukhamedov, *Direct Nuclear Reactions on Light Nuclei With Detected Neutrons* (FAN, Tashkent, 1978), pp. 7–49 (in Russian).

- [19] K.R. Greider and L.R. Dodd, Phys.Rev. **146**, 671 (1966).
- [20] N. Austern, R.M. Drisko, E.C. Halbert, G.R. Satchler, Phys.Rev. **133**, B3 (1964).
- [21] T. Berggren, Nucl. Phys. **72**, 337 (1965).
- [22] W.T. Pinkston, and G.R. Satchler, Nucl. Phys. **72**, 642 (1965).
- [23] L.D. Blokhintsev, E.I. Dolinsky, and V.S. Popov, Nucl. Phys. **40**, 117 (1963).
- [24] R.M. DeVries, Phys. Rev. C **8**, 951 (1973).
- [25] E.I. Dolinskii, and A.M. Mukhamedzhanov, Yad.Fiz. **3**, 252 (1966)[Sov. J. Nucl. Phys. **3**, 180 (1966)].
- [26] A. Azhari, V. Burjan, F. Carstoiu, H. Dejbakhsh, C.A. Gagliardi, V. Kroha, A.M. Mukhamedzhanov, L. Trache and R.E. Tribble, Phys.Rev. Lett. **82**, 3960 (1999).
- [27] A. Azhari, V. Burjan, F. Carstoiu, C.A. Gagliardi, V. Kroha, A.M. Mukhamedzhanov, X. Tang, L. Trache and R.E. Tribble, Phys.Rev. **60**, 055803 (1999).
- [28] G. Tabacaru, A. Azhari, J. Brinkley, V. Burjan, F. Carstoiu, Changbo Fu, C.A. Gagliardi, V. Kroha, A.M. Mukhamedzhanov, X. Tang, L. Trache, R.E. Tribble and S. Zhou, Phys.Rev. C **73**, 025908 (2006).
- [29] S.B. Igamov and R. Yarmukhamedov, Phys. At. Nucl. **71**, 1740 (2008).
- [30] O.R. Tojiboev, R. Yarmukhamedov, S.V. Artemov, S.B. Sakuta. Phys. Rev. C **95**, 054616 (2016).
- [31] C.A. Gagliardi, R.E. Tribble, A. Azhari, H.L. Clark, Y.-W. Lui, A.M. Mukhamedzhanov, A. Sattorov, L. Trache, V. Burjan, J. Cejpek, V. Kroha, S. Piskor, and J. Vincour, Phys. Rev. C **59**, 1149 (1999).
- [32] H. Lorenz-Wirzha, Ph.D. thesis, Universität, Münster, 1978.
- [33] H. Herndl, H. Abele, G. Staudt, B. Bach, K. Grün, H. Scsribany, H. Oberhummer, G. Raimann, Phys. Rev. C **44**, R952 (1991).
- [34] I. Lombardo, D. Dell'Aquila, A.Di Leva, I. Indelicato, M. La Cognata, M. La Commara, A. Ordine, V. Rigato, M. Romoli, F. Rosalo, G. Spadaccini, C. Spitareli, A. Tumino and M. Viliance, Phys. Lett. B **778**, 178 (2015).
- [35] P.O. Dzhamalov, and E.I. Dolinskii, Yad. Fiz. **14**, 753 (1971) [Sov. J. Nucl. Phys. **14**, 453 (1971)].
- [36] L.D. Blokhintsev, A.M. Mukhamedzhanov, R. Yarmukhamedov, Eur. Phys. J. A **49**, 108 (2013).

- [37] M. Abramowitz, I.A. Stegun, *Handbook of Mathematical Functions* (Dover, New York, 1970).
- [38] I.S. Gradshteyn, I.M. Ryzhik, *Tables of Integrals, Series, and Products*(Academic, San Diego, 1980).
- [39] D.A. Varshalovich, A.N. Moskalev, and V.K. Hersonskii, *Kvantovaya teoriya uglovogo momenta (Quantum theory of the angular momentum)*(Nauka, Leningrad, 1973)(in Russian).
- [40] K. Alder, D. Trautmann, *Ann. Phys.* **66**, 884 (1971).
- [41] Yu.A. Demkov, and V.N. Ostrovskii, *Zh. Exsp. Teor. Fiz.* **69**, 1582 (1975)[*Sov. Phys. JETP*, **69**, 806 (1975)].

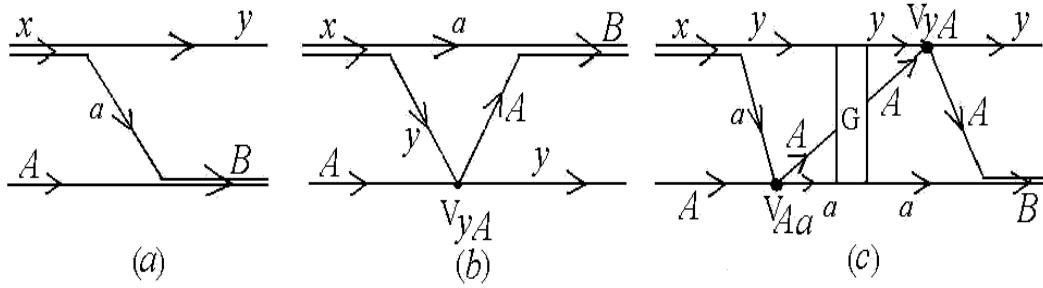


Figure 1: Diagrams describing transfer of the particle  $a$  and taking into account possible subsequent Coulomb-nuclear rescattering of particles ( $A$ ,  $a$  and  $y$ ) in the intermediate state.

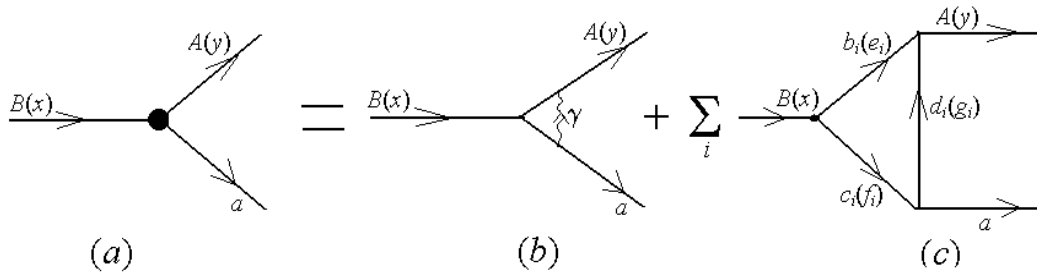


Figure 2: Diagrams describing the matrix element for the virtual decay  $B \rightarrow A + a$  ( $x \rightarrow y + a$ ).

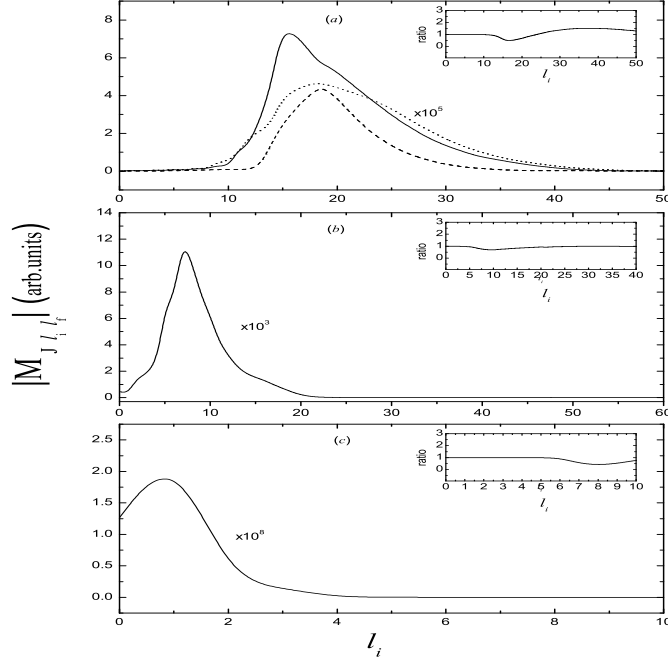


Figure 3: The  $l_i$  dependence of the modulus of the partial wave amplitudes ( $|M_{J l_i l_f}| \equiv |M_{l_x l_B J l_i l_f}^{\text{TBDW}}|$ ) for the  ${}^9\text{Be}({}^{10}\text{B}, {}^9\text{Be}){}^{10}\text{B}_0$  (a),  ${}^{16}\text{O}({}^3\text{He}, d){}^{17}\text{F}_0$  (b) and  ${}^{19}\text{F}(p, \alpha){}^{16}\text{O}$  (c) reactions at projectile energies of  $E_{10\text{B}}=100$  MeV,  $E_{3\text{He}}=29.75$  MeV and  $E_p=250$  keV, respectively, for which  $l_\alpha = l_{3\text{He}}=0$ ,  $l_{10\text{B}}=1$  and  $l_{17\text{F}_0}=2$  at different fixed values  $J$ . Here  $l_i$  and  $l_f$  are the relative orbital momenta in the entrance and exits channels of the considered reaction, respectively, and  $J$  is the transferred angular momentum. In (a), the solid line is for  $J=0$  and  $l_f = l_i$ , the dashed line is for  $J=1$  and  $l_f = l_i + 1$  and the dotted line is for  $J=2$  and  $l_f = l_i + 2$ . In (b), the solid line is for  $J=2$  ( $l_f = l_i + 2$ ). In (c), the solid line is for  $J=0$  ( $l_f = l_i$ ). The inserts are the ratio of the  $|M_{J l_i l_f}|$  calculated with taking into account of the renormalized Coulomb  $\mathcal{N}_{l_i l_f}^{\text{TBDM}}(E_i)$  factor to that calculated with  $\mathcal{N}_{l_i l_f}^{\text{TBDM}}(E_i)=1$  in the peripheral partial amplitudes (see Eqs. (48) and (49)).

Table 1: Reaction  $A(x, y)B$ ,  $F_C = F_C(\eta_x, \eta_B) = \Gamma(1 - \eta_x)\Gamma(1 - \eta_B)/\Gamma(1 - \eta_{xB})$  ( $\eta_{xB} = \eta_x + \eta_B$ ), incident energy  $E_x$ , values of renormalized CRFs  $\tilde{N}_{\text{pole}}^{\text{DW}}$  and  $\tilde{N}_{\text{post}}^{\text{DW}}$  as well as  $\tilde{N}^{\text{TBDM}}$  corresponding to the pole-approximation and the "post" form of DWBA as well as the exact three-body model, respectively, and quantities  $\mathcal{R}^{\text{TBDM}} = N^{\text{TBDM}}/N_{\text{pole}}^{\text{DW}} = \tilde{N}^{\text{TBDM}}/\tilde{N}_{\text{pole}}^{\text{DW}}$ ,  $\mathcal{R}_{\text{post}}^{\text{TBDM}} = N^{\text{TBDM}}/N_{\text{post}}^{\text{DW}} = \tilde{N}^{\text{TBDM}}/\tilde{N}_{\text{post}}^{\text{DW}}$ ,  $\mathcal{R}_{\text{post}}^{\text{DW}} = \mathcal{R}^{\text{TBDM}}/\mathcal{R}_{\text{post}}^{\text{TBDM}} = N_{\text{post}}^{\text{DW}}/N_{\text{pole}}^{\text{DW}} = \tilde{N}_{\text{post}}^{\text{DW}}/\tilde{N}_{\text{pole}}^{\text{DW}}$ .  $^{10}\text{B}_i$  denotes the ground ( $i=0$ ) state and the first-third ( $i=1-3$ ) excited ones of the residual  $^{10}\text{B}$  nucleus, while,  $^{17}\text{F}_i$  denotes the ground ( $i=0$ ) and first ( $i=1$ ) excited states of the residual  $^{17}\text{F}$  nucleus. Figures in the curly brackets are the modulus of the corresponding ratios.

$A(x, y)B;$ $\eta_B; \eta_{xB} (F_C)$	$E_x$ , MeV	$\tilde{N}_{\text{pole}}^{\text{DW}} (\tilde{N}_{\text{post}}^{\text{DW}})$	$\tilde{N}^{\text{TBDM}}$	$\mathcal{R}^{\text{TBDM}} (\mathcal{R}_{\text{post}}^{\text{TBDM}})$ [ $\mathcal{R}_{\text{post}}^{\text{DW}}$ ]
1	2	3	4	5
$^9\text{Be}(^7\text{Be}, ^8\text{B})^{10}\text{Be}$ 0.233; 1.823 (0.695)	84 [26]	$(9.222 - i\cdot 33.373)\times 10^3$ $((3.899 - i\cdot 14.112)\times 10^3)$	$-8.1648\times 10^4$	$-0.627 - i\cdot 2.292$ $(-0.374 - i\cdot 1.355)$ $\{1.671 + i\cdot 4.020\times 10^{-13}\}$ $\{1.67(1.46)[2.38]\}$
$^{14}\text{N}(^7\text{Be}, ^8\text{B})^{13}\text{C}$ 0.331; 1.921 (0.366)	85 [27, 28]	$(-7.865 + i\cdot 3.795)\times 10^3$ $((2.6553 - i\cdot 1.2813)\times 10^4)$	$-1.6084\times 10^4$	$16.58 + i\cdot 8.00$ $(1.47 - i\cdot 0.71)$ $[11.2 + i\cdot 2.1\times 10^{-11}]$ $\{18.4(1.63)[11.2]\}$
$^9\text{Be}(^{10}\text{B}, ^9\text{Be})^{10}\text{B}_0$ 0.234; 0.468 (0.871)	100 [8]	$0.339 - i\cdot 2.664$ $(0.515 - i\cdot 4.053)$	$-4.117$	$-0.193 - i\cdot 1.521$ $(-0.127 - i\cdot 1.000)$ $[1.521 + i\cdot 1.300\times 10^{-15}]$ $\{1.533(1.008)[1.521]\}$
$^9\text{Be}(^{10}\text{B}, ^9\text{Be})^{10}\text{B}_1$ 0.234; 0.482 (0.852)	100 [8]	$0.215 - i\cdot 2.833$ $(-0.333 - i\cdot 4.383)$	$-4.431$	$-0.118 - i\cdot 1.555$ $(-7.639\times 10^{-2} - i\cdot 1.005)$ $[1.546 - i\cdot 7.227\times 10^{-15}]$ $\{1.559(1.008)[1.546]\}$
$^9\text{Be}(^{10}\text{B}, ^9\text{Be})^{10}\text{B}_2$ 0.234; 0.506 (0.845)	100 [8]	$1.658\times 10^{-2} - i\cdot 3.147$ $(-2.643 - i\cdot 5.016)$	$-5.063$	$-8.476\times 10^{-2} - i\cdot 1.609$ $(-5.319\times 10^{-3} - i\cdot 1.009)$ $[1.593 + i\cdot 1.588\times 10^{-14}]$ $\{1.609(1.009)[1.593]\}$
$^9\text{Be}(^{10}\text{B}, ^9\text{Be})^{10}\text{B}_3$ 0.234; 0.519 (0.836)	100 [8]	$-7.489\times 10^{-2} - i\cdot 3.314$ $(-0.121 - i\cdot 5.361)$	$-5.417$	$3.691\times 10^{-2} - i\cdot 1.633$ $(2.281\times 10^{-2} - i\cdot 1.010)$ $[1.617 + i\cdot 1.405\times 10^{-14}]$ $\{1.634(1.010)[1.617]\}$
$^{16}\text{O}(^3\text{He}, d)^{17}\text{F}_0$ 1.577; 1.632 (0.983)	29.75 [31]	$261.48 + i\cdot 435.04$ $(279.68 + i\cdot 465.32)$	$-590.36$	$-0.599 + i\cdot 0.996$ $(-0.560 + i\cdot 0.932)$ $[1.069 - i\cdot 1.600\times 10^{-15}]$ $\{1.162(1.087)[1.069]\}$
$^{16}\text{O}(^3\text{He}, d)^{17}\text{F}_1$ 3.760; 3.815 (0.887)		$(-2.96 - i\cdot 4.75)\times 10^{15}$ $((-0.725 - i\cdot 1.160)\times 10^{15})$	$-1.33\times 10^9$	$(1.26 - i\cdot 2.05)\times 10^{-7}$ $((5.14 - i\cdot 8.26)\times 10^{-7})$ $[0.245 - i\cdot 1.300\times 10^{-11}]$ $\{2.406\times 10^{-7}(9.729\times 10^{-7})$ $[0.245]\}$

Table 2: continuation of Table 1

1	2	3	4	5
$^{19}\text{F}(p, \alpha)^{16}\text{O}(\text{g.s.})$ 0.585; 0.615 (0.943)	0.250 [32, 33]	$(-1.360 + i \cdot 0.453) \times 10^{-3}$ $((-1.48 + i \cdot 0.494) \times 10^{-3})$	$-1.68 \times 10^{-3}$	$1.112 + i \cdot 0.370$ $(1.023 + i \cdot 0.340)$ $[1.088 - i \cdot 7.150 \times 10^{-18}]$ $\{1.172(1.078)[1.088]\}$
	0.350	$(-3.20 + i \cdot 1.14) \times 10^{-3}$ $((-3.480 - i \cdot 1.240) \times 10^{-3})$	$-3.98 \times 10^{-3}$	$1.104 + i \cdot 0.394$ $(1.014 + i \cdot 0.361)$ $[1.088 - i \cdot 6.005 \times 10^{-18}]$ $\{1.172(1.076)[1.088]\}$
	0.450	$(-5.41 + i \cdot 2.04) \times 10^{-3}$ $((-5.893 - i \cdot 2.217) \times 10^{-3})$	$-6.78 \times 10^{-3}$	$1.097 + i \cdot 0.412$ $(1.008 + i \cdot 0.379)$ $[1.088]$ $\{1.172(1.077)[1.088]\}$
	0.327 [34]	$(-2.750 + i \cdot 0.97) \times 10^{-3}$ $((-3.00 + i \cdot 1.05) \times 10^{-3})$	$-3.42 \times 10^{-3}$	$1.110 + i \cdot 0.390$ $(1.020 + i \cdot 0.360)$ $[1.090]$ $\{1.177(1.082)[1.088]\}$
	0.387	$(-3.980 + i \cdot 1.450) \times 10^{-3}$ $((-4.330 - i \cdot 1.580) \times 10^{-3})$	$-4.97 \times 10^{-3}$	$1.100 + i \cdot 0.400$ $(1.010 + i \cdot 0.370)$ $[1.090]$ $\{1.170(1.076)[1.090]\}$
	0.486	$(-6.30 + i \cdot 2.41) \times 10^{-3}$ $((-6.850 + i \cdot 2.62) \times 10^{-3})$	$-7.90 \times 10^{-3}$	$1.090 + i \cdot 0.420$ $(1.010 + i \cdot 0.380)$ $[1.090]$ $\{1.168(1.079)[1.090]\}$

Table 3: The specific reactions and the corresponding to them vertices described by the triangle diagram Fig. 2c, the positions of singularities  $i\kappa$  and  $i\kappa_i$  ( $i\bar{\kappa}_i$ ) in  $q_{Aa}(q_{ay})$  as well as  $\xi$  and  $\xi_i$  ( $\bar{\xi}_i$ ) in the  $\cos\theta$ -plane of the reaction amplitude, where  $\kappa$  is related either to the vertex  $B \rightarrow A+a$  ( $\kappa = \kappa_{Aa}$ ) or to the vertex  $x \rightarrow y+a$  ( $\kappa = \kappa_{ya}$ ).

Reaction $A(x, y)B$	$E_x^{\text{lab}}$ MeV	The vertex		$\xi$ ( $\kappa$ , fm $^{-1}$ )	$b_i$ ( $e_i$ )	$c_i$ ( $f_i$ )	$d_i$ ( $g_i$ )	$\kappa_i(\bar{\kappa}_i)$ , fm $^{-1}$	$\xi_i$ ( $\bar{\xi}_i$ )
		$B \rightarrow A + a$ ( $x \rightarrow y + a$ )							
${}^9\text{Be}({}^{10}\text{B}, {}^9\text{Be}){}^{10}\text{B}_0$	100	${}^{10}\text{B}_0 \rightarrow {}^9\text{Be} + p$	1.020(0.534)	${}^8\text{Be}$	$d$	$n$	0.940	1.064	
				${}^6\text{Li}$	${}^4\text{He}$	$t$	2.024	1.479	
				$n$	${}^9\text{B}$	${}^8\text{Be}$	0.802	4.169	
${}^{16}\text{O}({}^3\text{He}, d){}^{17}\text{F}_0$	29.7	${}^{17}\text{F}_0 \rightarrow {}^{16}\text{O} + p$	1.065(0.165)	${}^{14}\text{N}$	${}^3\text{He}$	$d$	2.696	3.253	
				${}^{13}\text{N}$	${}^4\text{He}$	$t$	2.645	3.508	
				$p$	${}^{16}\text{O}$	${}^{15}\text{N}$	0.905	49.551	
					$({}^3\text{He} \rightarrow d + p)$		1.065( 0.420)	$(p)$	$(d)$
${}^{19}\text{F}(p, \alpha){}^{16}\text{O}$	0.250	${}^{19}\text{F} \rightarrow {}^{16}\text{O} + t$	13.648(1.194)	${}^{15}\text{N}$	${}^4\text{He}$	$p$	1.522	19.720	
	0.350						1.522	16.647	
	0.450						1.522	14.665	